University of Natural Resources and Life Sciences, Vienna

DNA and endotoxin removal from *E. coli* homogenate

Alexander Jurjevec, B.Sc.

Master Thesis

in partial fulfilment of the requirements for the degree of

Diplom-Ingenieur

Department of Biotechnology

University of Natural Resources and Life Science, Vienna

Department Head: Univ.Prof. Dipl.-Ing. Dr.rer.nat. Reingard Grabherr

Supervisor: Assoc. Prof. Dipl.-Ing. Dr. Rainer Hahn

Acknowledgement

I would like to thank my Supervisor Rainer Hahn for his help and valuable input, without which it would not have been possible to complete this Master Thesis. The opportunity to deal with this challenging work has given me a lot of theoretical as well as practical knowledge. I would also like to express a special thanks to my working group members, who gave me valuable input in practical work.

Zusammenfassung

Der Einfluss von DNA und Endotoxin auf die Reinigung des cytoplasmatischen grün fluoreszierenden Proteins (GFP) von *E. coli* Homogenaten wurde untersucht. Die Reinigung beinhaltete Hochdruck-Homogenisierung, Hitzebehandlung der Homogenate (50°C, 3h) und Flockung mit Polyethyleneimine PEI (10 kDa, verzweigt). Ein besonderer Focus wurde auf das Adsorptionsverhalten von GFP, DNA und Endotoxin auf einem Anionenaustauscher gelegt. Homogenisierungsbedingungen hatten dabei einen signifikanten Einfluss auf die von der Zelle freiwerdenden DNA- und Endotoxin Moleküle. Die Hitzebehandlung des Homogenats führte zu einer höheren Reinheit der Proteinlösung und zu einer Reduktion der DNA- und Endotoxinkonzentration zu 10% bzw. 50%. PEI führte zusätzlich zu einer starken Reduktion der DNA- und Endotoxinkonzentration und 0.2% PEI (m/v) waren ausreichend, um die meisten DNA- und Endotoxin Moleküle abzureichern. Das Adsorptionsverhalten von GFP, DNA und Endotoxin wurde mit Batch-Adsorptionsversuchen und Durchbruchskurven auf einer Chromatographiesäule evaluiert. Die Adsorptionsisothermen zeigten bei den diafiltierten-Homogenaten und hitzebehandelten Homogenaten eine Verdrängung von GFP bei höheren Proteinkonzentrationen. Diese Verdrängung zeigte sich, als die Bindungskapazität von DNA und Endotoxin anstieg. Es wurde vermutet, dass diese beiden Komponenten für die Verdrängung verantwortlich sind. Im Gegensatz dazu, zeigten die PEI behandelten Proben hochaffine Isothermen mit höherer Bindungskapazität. In Batch-Adsorptionsversuchen wurde gezeigt, dass DNA und Endotoxine sehr schnell adsorbieren, währen die Verdrängung von GFP eine langsame Reaktion ist. Die Durchbruchskurven wurden mit einem Adsorptionsmodell für Film- und Porendiffusion evaluiert. Die hitze- und PEI behandelten Proben zeigten dabei eine höhere Bindungskapazität sowie einen besseren Massentransfer. Sowohl Film-, als auch Porendiffusion waren deutlich schneller.

Abstract

The influence of DNA and endotoxins on the purification of cytoplasmatic green fluorescent protein (GFP) from *E. coli* was investigated. Purification included high pressure homogenisation (HPH), heat-treatment of homogenates (50°C, 3h) and flocculation with polyethyleneimine PEI (10 kDa branched). A special focus was the adsorption behaviour of GFP, DNA and endotoxin on an anion exchange resin which was used as capture step. It was found that different operating conditions in HPH had significant influence on DNA and endotoxin release from the cells. Heat-treatment of homogenates led to higher purity of protein solution and a reduction to 10% of initial DNA- and to approximately 50% of initial endotoxin concentration. PEI led to additional strong reduction of DNA and endotoxins and at 0.2% PEI (w/v) most of DNA and endotoxins were depleted. Adsorption behaviour of GFP, DNA and endotoxins were evaluated with batch adsorption and column break-through experiments. Adsorption isotherms showed a displacement of GFP at higher protein concentration for diafiltrated- homogenate and heat-treated homogenate. The displacement occurred when binding capacity of DNA and endotoxin started to increase, indicating their potency as displacer. In contrast, PEI treated samples showed highly favourable adsorption isotherms with increased binding capacity. Batch adsorption experiments showed, that initial adsorption of DNA and endotoxin is very fast, while displacement of GFP is a very slow reaction. Break-through experiments were evaluated an adsorption model for film and pore diffusion. PEI flocculation in combination with heat-treatment not only led to a high increase of binding capacity but also to increased mass transfer. It was shown that both, pore diffusion as well as film diffusion were significantly enhanced.

Contents

1. Introduction

The gram negative enterobacterium Escherichia coli is a widely used microorganism that has already been intensively studied. Due to its` rapid growth, high yield of product and cost-effectiveness, *E. coli* is the first-choice microorganism for the production of heterologous proteins including biopharmaceuticals. [1] [2]. Even though there is the detailed knowledge about the genetics and metabolic levels, heterologous proteins produced by *E. coli* are not secreted to the extracellular space due to the cytoplasmatic- and outer membrane of the *E. coli* cells. Various investigation have been made to find secretion strategies for *E. coli* for instance by using a leader sequence. However these strategies are difficult to apply and not broadly applicable [3]. Therefore, for the purification of intracellular protein production a cell lysis or cell disruption method is necessary. Mechanical cell disruption methods like high pressure homogenisation (HPH) are broadly used at industrial scale but they are not selective. This means that through this method not only the desired recombinant proteins are released into the supernatant, but also other host cell components. Neidhardt et al. [4] have determined the typical dry weight composition of an *E. coli* cell with 55% Protein, 2.5% Glycogen, 3.4% Lipopolysaccharides, 2.5% Murein, 20.5% RNA, 3.1% DNA, 9% Lipid and 3.9% Metabolites and Ions. This makes the starting material for the purification of each recombinant protein produced in *E. coli* complex, heterogeneous and potentially unsafe. Potentially dangerous impurities in E.coli cells are for instance DNA and Endotoxins [5]. Therefore several unit operation steps are necessary to purify recombinant proteins out of an *E.coli* homogenate including primary recovery steps like centrifugation, ultra- and diafiltration. The use of alternative purification methods like heat-precipitation and flocculation but also capture and polishing steps with chromatographic methods. In this investigation, the influence of DNA and Endotoxin on the purification of GFP out of an *E.coli* homogenate was observed. One focus was set onto the tracking of DNA and Endotoxin levels using different homogenisation conditions, the influence of an additional heat-precipitation- and an additional flocculation step on the DNA and Endotoxin levels using Polyethyleneimine. In further consequence the adsorption behaviour of GFP, DNA and Endotoxin on an anionic exchange capture step was investigated which is of great interest due to their properties i.e. size and negative charge. It was not the goal to obtain an Endotoxin- and DNA free GFP solution.

1.1 Properties of Host Cell Components

1.1.1 DNA

Although DNA encode the genetic information, in the production of protein pharmaceuticals both, genomic and plasmid DNA has to be seen as a product impurity and potential risk due to concerns about the possibility for cellular transformation by potentially oncogenic DNAs. Therefore the World Health Organization recommend a maximum of 10 ng per dose of cellular DNA for biopharmaceutical products used for injection [5][6][7].

DNA is composed of four nucleotides, i.e. the two purine bases adenine and guanine and the two pyrimidine bases thymine and cytosine. Each of this bases contain a sugar group, the deoxyribose with a phosphate residue. In DNA the nucleotides are arranged in a double-stranded helical structure. Adenine (A) pairs with Thymine (T) and Cytosine pairs with Guanine (G) by forming hydrogen bonds. [5][8]. Figure 1shows the structure of DNA (from [10])
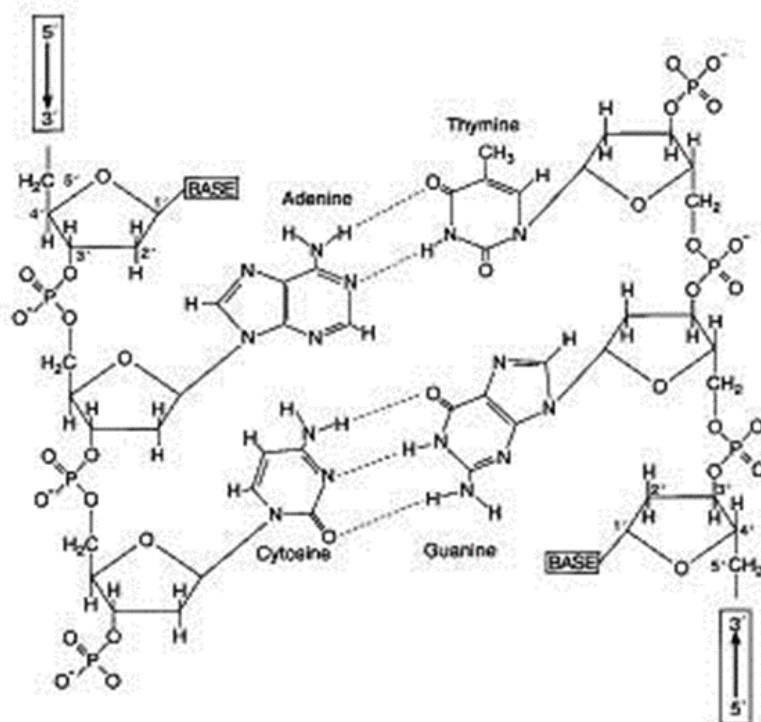
Figure 1: Structure of DNA

The arrangement of DNA in *E. coli* can be subdivided into two different forms: genomic and plasmid DNA. The genomic DNA is arranged in one free chromosome and organised in a compact form called nucleoid. The nucleoid is a closed duplex structure with a serial of loops. These DNA loops are "negatively supercoiled" which leads to further compaction [9].

11

Figure 2 shows a schematic supercoiled structure of an *E. coli* chromosome [10].
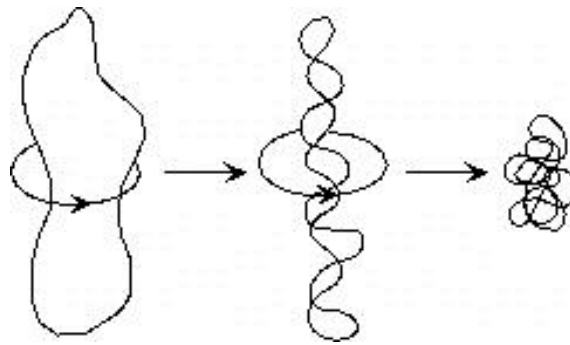
Figure 2: DNA arrangement in E. coli

The plasmid DNA is an entity which replicates independently of the genomic DNA in the bacterial cytoplasm. Plasmid DNA can exist in different forms including supercoiled, circular linear and aggregated. The size and the number of plasmids varies within the bacterial cell. [5][9].

Nucleotides are hydrophilic and negatively charged over a wide range of pH due to their exposed phosphate groups. In physiological solution, DNA exists in a wide range of molecular mass ranging from 10- to 10000 kDa. The diffusivity in dilute solution is very slow with approximately 10^{-9} cm^2 s^{-1} and is valid for larger DNA molecules. The stability of dsDNA is mainly affected by hydrogen bonds between the base pairs and pi-stacking, a non-covalent interaction that occurs only between the aromatic portions of bases. Since GC forms three hydrogen bonds, the higher the GC content in the base sequence, the higher the stability [5][9][11].

1.1.2 Endotoxins

A major issue with the expression of proteins in *E. coli* host cells are endotoxins, which are also referred to as lipopolysaccharides (LPS). The terminus endotoxin is known for more than 100 years and was chosen by Robert Pfeifer to distinguish endotoxins from bacterial exotoxins such as the botulinum toxin. Endotoxins are an integral part of the outer cell membrane which are responsible for organisation and stability. Although endotoxins are anchored in the cell wall, they are continuously released into the surrounding medium. Even very small concentrations of endotoxin in the bloodstream can lead to a systemic inflammatory reaction, such as endotoxin shock, tissue injury and death.[12][13][14]. Therefore, the European Pharmacopeia set the limit for intravenous application to 5 endotoxin units (EU) per kg body weight and hour. The term EU describes the biological activity of an endotoxin. As a rule of a thumb 1 EU corresponds to 100 pg of endotoxin. Figure 3:shows the schematic chemical structure of endotoxins according to Ohno and Morrison [15].
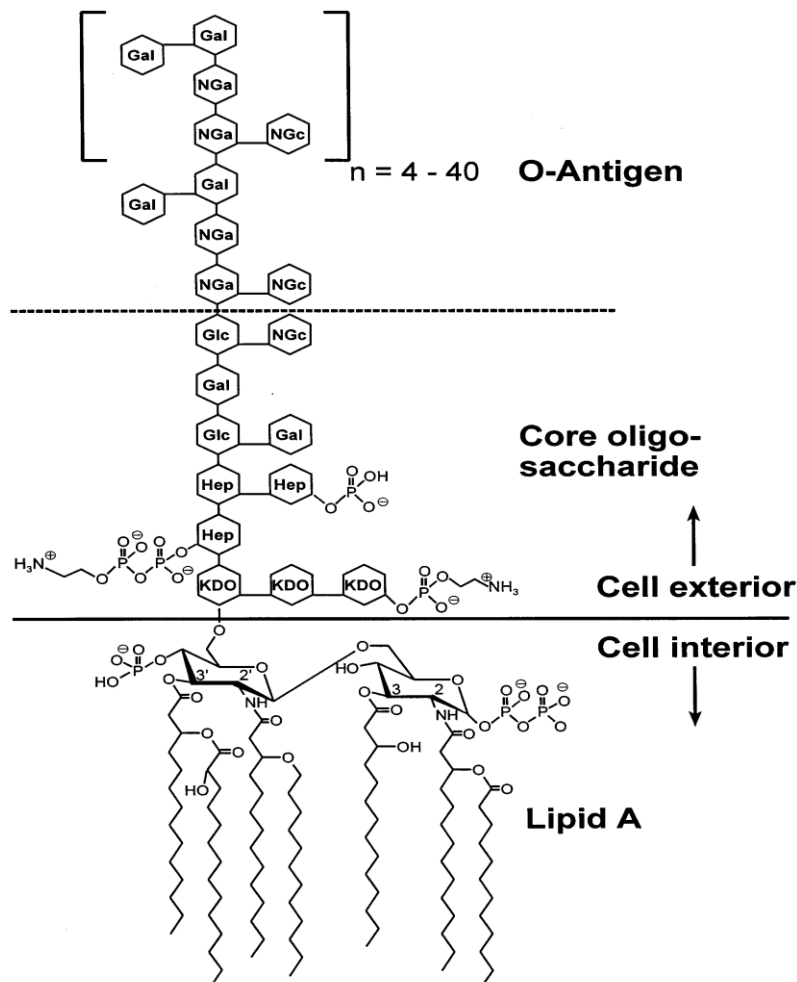
Figure 3: Schematic view of the chemical structure of endotoxin from E. coli O111:B4. Hep, L-glycero-D-manno-heptose; Gal, galactose; Glc, glucose; KDO, 2-keto-3-deoxyoctonic acid; NGa, N-acetyl-galactosamine; NGc, N-acetyl-glucosamine

The chemical structure of endotoxins can be subdivided into three parts. Lipid A is the highly hydrophobic and endotoxically active part of the molecule. It is the most conserved part of the endotoxin molecule. It consist of a β-1,6-linked D- glucosamine residue which is covalently linked to 3-hydroxy-acyl substituents with 12-16 carbon atoms via amide or ester bonds. These can be further esterified with saturated fatty acids [16][17]. The core oligosaccharide can be subdivided into the outer- and inner core. The inner core is attached to the Lipid A and consists of the unusual sugars 2-keto-3-deoxyoctonic acid and L-glycero-D-manno-heptose. The outer core which extends further from the bacterial cell surface consists more common sugars like galactose, glucose, N-acetyl-galactosamine and N-acetyl-glucosamine. On the outer core, the O-polysaccharide is attached which is often referred as O-antigen because it is the major antigen targeted by the immune response of the host. The O-polysaccharide is built up of repeating oligosaccharide units including galactose, glucose, N-acetyl-galactosamine and N-acetyl-glucosamine [17].

Lipid A is phosphorylated and partially phosphorylated. Therefore endotoxins exhibit a net negatively charge in solutions. The molar mass of an endotoxin monomer is about 10- 20 kDa however, endotoxins form aggregates of high stability with molecular weights of more than 1000 kDa. It is assumed, that these aggregates are formed by non-polar interactions between neighbouring alkyl chains as well as bridges between phosphate groups and bivalent cations. This leads to lamellar, cubic and hexagonal arrangements such as micelles and vesicles with diameters up to 0.1 μm. The actual arrangement of endotoxin monomers cannot be predicted and depends on the properties of the solution. Therefore it is also possible that when protein shifts equilibrium, endotoxin monomers could release from aggregate. Figure 4gives an overview of the possible arrangements of endotoxins in solution[18][19][20].
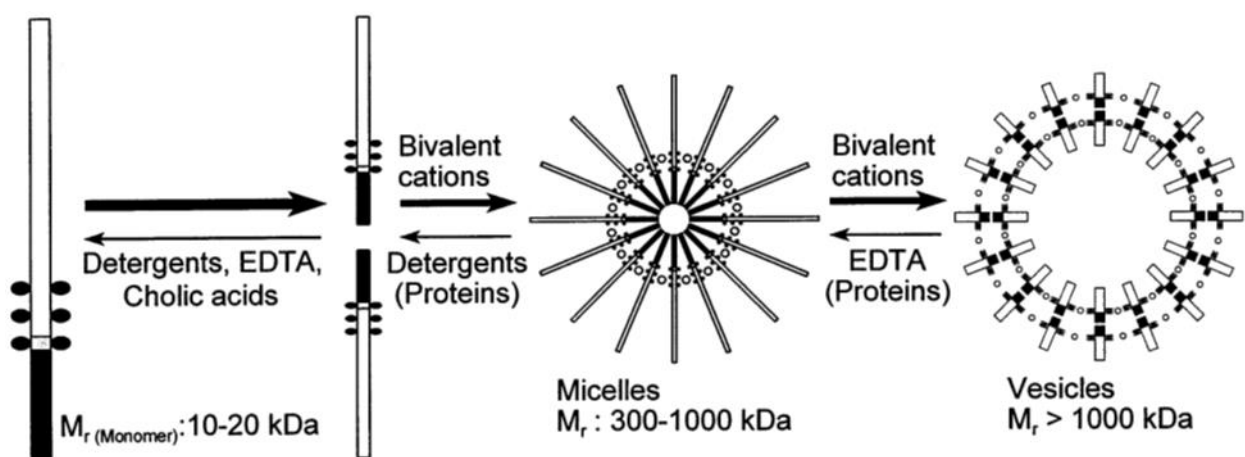
Figure 4: Arrangements of Endotoxins in solution

1.1.3 GFP

Green Fluorescent Protein GFP was discovered by Shimomura et al [21][22] as a companion protein to aequorin, the chemiluminescent protein from Aequorea jellyfish. They published the emission spectrum of GFP, which peaks at 508 nm. It was noted that the green bioluminescence of living Aequorea tissue also peaks close to this wavelength, whereas the chemoluminescence of pure aequorin was blue and peaks at around 470 nm, which is close to one of the excitation peaks of GFP.

GFP is intrinsically fluorescent, has a low toxicity, is very resistant to denaturation and allows easy imaging and quantification. This makes GFP broadly applicable. GFP is successfully used as a reporter gene, as active indicator or as fusion tag since it does not alter the function and localisation of the fusion partner. The GFP wild type consists of 238 amino acids which are folded in 11 β-strands with a central α- helix and has a molecular weight of about 27 kDa. GFP chromophore is a cyclic tripeptide forming a p,- hydroxyl-benzyl-idene-imidazolinone derived structure from residues 65-67, which are Ser-Tyr-Gly in the native protein. Due to drawbacks of the wild type GFP like its` low fluorescence intensity and display of multiple absorption and emission maxima, many mutants were developed with increased stability and intensity [23].

The GFPmut3.1 which is used in this study is a variant of the Aequorea GFP. This variant displays a very bright green fluorescence when expressed in bacteria because its` mutations where Ser-65 is substituted by Glycine and Ser-72 to Alanine. This leads to an increase in the efficiency of protein folding and chromophore formation at 37°C [24].

1.2   Methods for primary recovery and purification

1.2.1 High Pressure Homogenisation

The first step in the recovery of intracellular proteins from E. coli is a cell- disruption or lysis method[25]. A widely used disruption method is high pressure homogenisation (HPH). In the HPH, a cell suspension is pumped through a narrow orifice between the valve seat and the valve as shown in Figure 5 [26] [27].
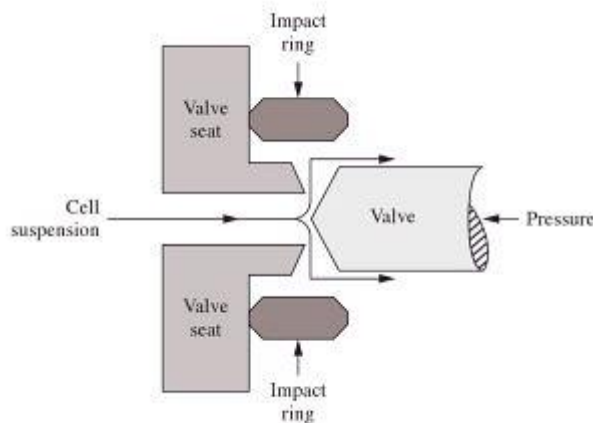
Figure 5: Valve of a High Pressure Homogeniser

The cell suspension is accelerated in this minute orifice and decelerated at the impact ring. The space between the valve and the valve seat is often the only operating variable that can be varied. Decreasing the space between the valve and the valve seat will increase the operating pressure. Homogeniser are available as single- and two stage devices, where the first stage is used to apply the whole inlet pressure. The second stage creates the back pressure and also reduces the noise and vibration of the outlet pipe [28]. There are several investigations about the responsible forces which lead to the breakage of the bacterial cell walls. These are hydrodynamic forces such as inlet pressure gradient, channel shear stress, post channel turbulence and impact ring impingement forces. There is also the theory that cavitation is a parameter that is responsible for cell breakage. R. Lander et al [29] show the potential contribution of cavitation by applying back pressure. The applied back pressure leads to a reduction of the molecular weight reduction compared to when no back pressure is applied. They stated, that the cavitation occurs at the impingement and is suppressed by the applied back pressure. The applied back pressure has also impact on the protein release properties of the homogenate. Zartler [30] showed that an applied pressure of 500 bar in the first stage and 50 bar in the second stage lead to a higher protein release compared to 500

bar in the first- and 0 bar in the second stage and consequently assumed, that the instant pressure drop to zero bar increases the mechanical stress and damage the protein.

Because the desired degree of cell disruption and product release generally is not achieved during a single passage through the homogeniser, multiple passages are required. According to Wong et. al [31], it is favourable to apply less pressure but perform more passages. Zartler [30] showed that, with more than one passage, the viscosity of the homogenate decreases due to DNA fragmentation in the homogenisation process. The degree of disruption is described by Equation 1.

$$\ln\left(\frac{R_{max}}{R_{max} - R}\right) = kNp^{\alpha}$$

R_{max} is the maximum amount of protein available for release. R is the amount of protein released after N passes through the homogeniser, k is a temperature dependent rate constant, and p is the operating pressure. α is a measure of the resistance of the cells to disrupt; values of α range between 0.9 and 2.9 for bacteria and yeast. Both k and α vary with cell type. According to this equation operating on the maximum pressure will produce the maximum number of broken cells and maximize the release of the desired product. However, this can lead to some negative effects like thermal degradation due to the heat of the homogenizer or the formation of small cell debris which interferes with the downstream isolation process [32].

1.2.2 Flocculation

Bioparticles like bacterial cells or cell debris, generated by cell lysis are negatively charged in aqueous solutions. As two particles approach each other, they interact via repulsive- and attractive forces as shown in Figure 6.
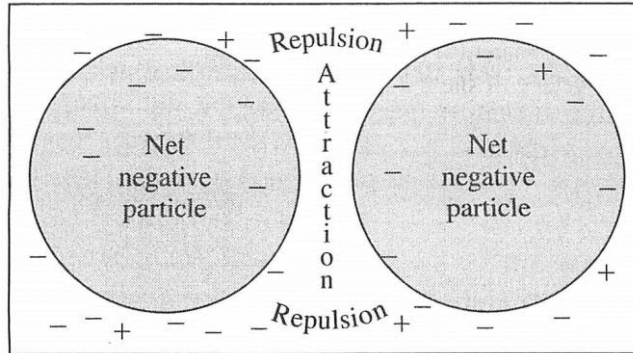
Figure 6: Bioparticles in aqueous solution

Flocculation is the attachment of suspended particles to one another when van der Waals interactions, which are attractive forces between nonpolar particles, are not counteracted by electrostatic repulsion and is therefore related to the electrokinetic properties of particles and molecules. The typical objective is to reduce the electrical repulsion force as much as possible so that the attractive van der Waals force is higher than the electric repulsion. This is described by the DLVO theory [33] and most flocculations happen due attachments between particles in the secondary minimum as shown in Figure 7.
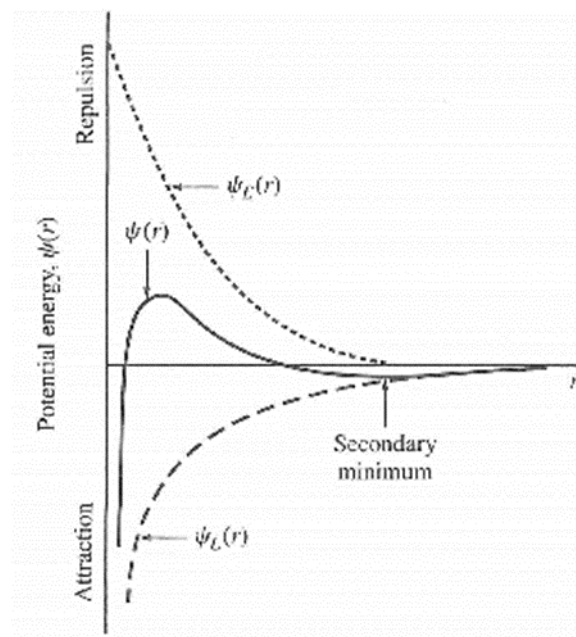
Figure 7: Potential energy between two like charged particles

Figure 7 shows the potential energy between two like-charged particles separated by the distance r, where ΨE (r) is the repulsive double layer potential and ΨL (r) is the attractive potential due to London and van der Waals forces. The two curves are summed up in the Ψ (r) and are less than zero in the secondary minimum.

Poly-ionic polymers like Polyethyleneimine can be used as electrolytes in flocculation by a mechanism called polymer bridging. They confer a positive charge on the negative bio-particles, causing the bio-particle to become electrostatically attractive to the double layers of colliding particles. A single cationic polymer can neutralize the negative charges of a bio-particle surface and also can attract more than one particle simultaneously by electrostatic forces. This is shown in Figure 8.The effectiveness of the polymer depends molecular weight, charge, solubility and their interactions with particles depends on pH, ionic strength, temperature and solid concentration [34].
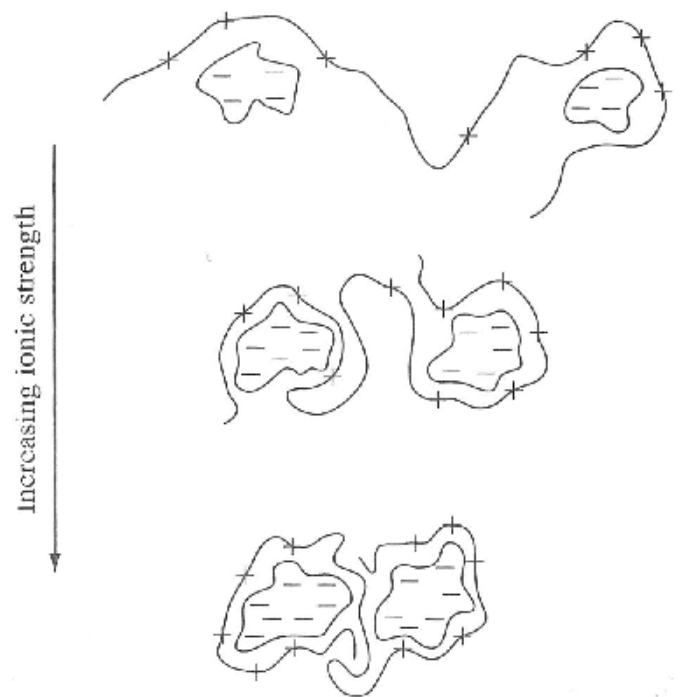
Figure 8: Polymer bridging of bio-particles

1.2.3 Heat Precipitation

The aggregation of proteins is separated into two distinct parts. In the first, the protein is unfolded and as temperature is increased denaturation will occur at some point. In the second part the denatured protein is aggregated [34][5]. The simplest case for denaturation is the two state model for reversible denaturation:

N ↔ U
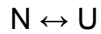
Where N represent the native- and U represent the unfolded state. However, most of the proteins and especially intracellular proteins do not show reversible denaturation. For those a three-state model which is expanded to the irreversible state D is more accurate. The main mechanism for irreversible denaturation is aggregation [35].

N ↔ U → D

The process of denaturation is greatly accelerated by a rise of temperature.[36] Gosh and Dill found that a temperature shift from 37 °C to 41 °C is sufficient to denature 20% of the *E. coli* proteins and predicted a thermal death point between 49 – 55 °C [37]. But some of the *E. coli* proteins are stable this kind of heat exposure. Kwon et al. have identified 17 heat stable proteins in *E.coli* [38].

Nevertheless, the circumstance that most host cell proteins are not stable to heat exposure can be used to facilitate the purification of recombinant heat stable proteins. Fink observed in his thesis, that in the purification of the heat stable Green fluorescent protein, a pre- treatment of *E. coli* homogenate with 50 °C for 3 hours leads to a high increase in turbidity and solid content indicating the aggregation of host cell proteins and cell debris. He also observed increasing particle diameter of the aggregates and therefore a higher clarification efficiency in the following centrifugation step.[39].

The thermal stability of DNA depends on the size of the DNA fragments and their arrangement in solution. Typical melting temperatures T_m of DNA fragments, the temperature at which half of the DNA is denatured are between 50- 100 °C. The DNA can also renature under these temperatures but a part will be irreversible degraded by long time exposure to these temperatures [40][41].

Endotoxins are extremely resistant to temperature due to their amphiphatic structure. Endotoxins can only be inactivated when exposed to a temperature of 250°C for more than 30 min or 180°C for more than 3 h with dry-heat [42][43]. Therefore it is assumed, that heat treatment without destroying the desired protein will not influence the endotoxin level of the starting suspension.

1.2.4 Centrifugation

Centrifugation is a widely used method to separate materials of different densities by the application of a force greater than gravity. In the area of biotechnology, it is for instance used for the removal of cells from fermentation broths or for the cell debris removal after homogenisation. Settling velocity in a gravitational field is described by Stoke`s law shown in Equation 2:

$$u_g = \frac{\rho_P - \rho_L}{18\mu} D_P^2 g$$

Equation 2: Settling velocity in gravitational field

In this formula u_g is the sedimentation velocity in a gravitational field, ρ_p is the density of the particle, ρ_L is the density of the liquid, μ is the viscosity of the liquid, Dp is the particle diameter, and g is gravitational acceleration. In a centrifuge the gravitational acceleration g is replaced by the angular velocity ω^2 times the radius of the centrifuge drum leading to the velocity of a particle in the centrifuge u_c shown in Equation 3 [27]:

$$u_c = \frac{\rho_P - \rho_L}{18\mu} D_P^2 \omega^2 r$$

Equation 3: Settling velocity in accelerated field

1.2.5 Membrane Filtration

In general, filtration is used to separate solutes or solid components in a fluid suspension based on their size difference. The driving force is the transmembrane pressure Δp, which is built up across the membrane. The transmembrane pressure can be calculated according to Equation 4, where p_i is the inlet pressure of the feed medium, p_o is the outlet pressure and p_p is the permeate pressure.

$$\Delta p = \frac{p_i + p_o}{2} - p_p$$

Equation 4: Transmembrane pressure in filtration process

A key parameter for the characterization of a membrane filtration process is the permeate flux J_p. The permeate flux is defined as the as the volumetric permeate flow F_p per area of membrane A shown in Equation 5.

$$J_p = \frac{F_p}{A}$$

Equation 5: Determination of Permeate flow

According to the direction of the fluid feed, a distinction is made between dead- end filtration and crossflow filtration.

In dead-end filtration a suspension flows against a filter medium vertically by the application of a pressure gradient across the filter medium. The solids in the suspension are retained on the filter medium and are building a layer, the so-called cake. The thickness of the cake is responsible for the flow through the filter medium. The thicker the cake the lower the flow.

In cross flow filtration a suspension flows parallel to the membrane surface. The particles which are bigger than the pores of the membrane are retained whereas the smaller particles can pass through the membrane pores. The pore size is generally characterized by the nominal cut off which is given as molecular weight in kilo Dalton, where 90% of the globular proteins are retained by the membrane. Typical applications in downstream processing are product ultrafiltration and diafiltration. Aim of ltrafiltration is the concentration by reduction of the volume of a protein solution to avoid high buffer consumption for the following diafiltration step. The diafiltration is used to replace the solvent or buffer of the actual protein solution. The main application of diafiltration is to prepare protein solution prior to or in between chromatographic steps. Figure 9 gives a schematic overview of ultra- and diafiltration.

In an ultrafiltration process a protein solution is pumped across the membrane area. The proteins and other macromolecular components above the cut off of the membrane are retained and transported back to the reservoir tank. Low molecular weight components below the cut off pass through the membranes pores and are collected in a separate tank. This is called permeate. The desired concentration of the protein solution can be controlled by the permeate volume.

In diafiltration, a constant amount of buffer is added to the protein solution. Thereby the amount of the added buffer is equal to the removed permeate volume. The amount of buffer exchanged can be controlled by conductivity measurement of the retained protein solution[27][34][30][44].
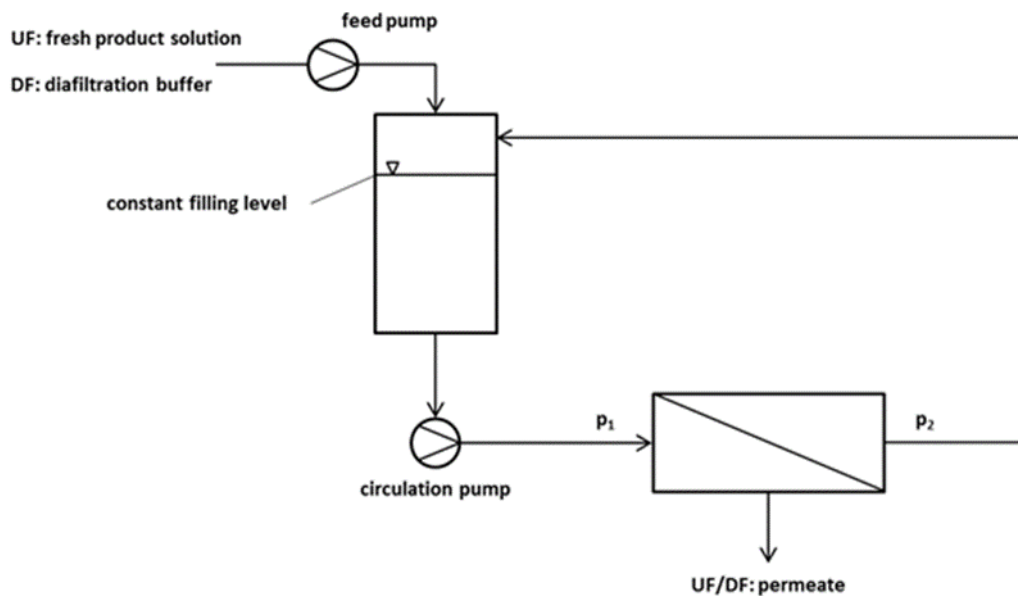

Figure 9: Schematic ultra- and diafiltration process

1.2.6 Ion Exchange Chromatography

Chromatography is based on the principle, that a mixture of components can be separated, when they are transported in a fluid phase through a fixed-bed interacting material. The fluid phase is defined as the mobile phase whereas the fixed-bed interacting material is defined as the stationary phase. Typically, the stationary phase is composed of liquid-filled porous bead-shaped particles with functional ligands. The particles are available in different sizes and vary from smaller than 2 µm for analytical purposes up to 200 µm for preparative operations. The morphology of a particle is determined by the particle porosity which is the relation of the liquid filled pores and the total volume of the particle. Since the surface area within the pores is much higher than the outer surface of the particle, diffusional mass transfer is the dominating mechanism for protein adsorption on porous particles.

The ion exchange chromatography is the most frequently used chromatography method. It`s principle is based on electrostatic interaction and binding occurs between charged groups of the molecule and oppositely charged ligands which are immobilized on a surface. Proteins exhibit a charge depending on their acidic- and basic amino acid residues and the carboxyl terminus of the polypeptide chain. The net charge of proteins depends on ionisable amino acid residues and their pKa values and it changes with pH. When the pH is about two units above the pKa values the acidic amino acid residues become completely deprotonated whereas the basic amino acid residues become completely protonated when the pH is about two units below the pH. At a certain pH, the proteins exhibit a net charge of zero. This is called the isoelectric point pI where the acidic- and basic amino acid residues are equally balanced. Proteins with a negative charge bind to an anion exchanger, whereas proteins with a positive charge bind to a cation exchanger. The adsorbed proteins can be eluted by increasing the ionic strength i.e. by increasing the salt concentration. Alternatively, proteins can be eluted by changing the pH.

1.2.7 Adsorption equilibria

The concentration of adsorbed protein in the stationary phase in equilibrium with the mobile phase is expressed by adsorption isotherms. A model which is often used to describe the protein adsorption is the Langmuir isotherm model for single component adsorption shown in Equation 6:

$$q = \frac{q_m KC}{1 + KC}$$

Equation 6: Langmuir isotherm model for single component adsorption

q_m is the maximum binding capacity (mg/mL resin), C is the protein concentration (mg/mL) in the fluid phase and K is an equilibrium constant (mL/mg). The Langmuir isotherm can also be written by a dimensionless separation factor R in Equation 7:

$$R = \frac{1}{1 + KC_{ref}}$$

Equation 7: Langmuir isotherm as dimensionless separation factor

C_{ref} is usually the initial concentration of protein. The isotherm is linear if R = 1, favourable for R < 1 and rectangular for R > 1. In general a linear relationship between adsorbed protein and free protein in solution can be observed at low protein concentrations. With increasing protein concentration, a non- linear behaviour can be observed which ends up in the maximum binding capacity. The maximum binding capacity is dependent on the available surface area and the concentration of binding sites.

Considering bioseperation processes, it is obvious that single component adsorption is usually not the case especially in capture steps, where the proteins are separated out of fermentation broths or homogenates. The extension of the Langmuir isotherm in Equation 8 for a multicomponent system for N- adsorbed is practically used to describe this adsorption behaviour:

$$q_i = \frac{q_{m,i} K_i C_i}{1 + \sum_{j=1}^{N} K_j C_j}$$

Equation 8: Extension of Langmuir isotherm model for multicomponent systems

A simple method to design an experimental setup that covers the full concentration range can be seen in Equation 9:

$$V = \frac{\frac{C q_m K_a}{1 + K_a C} V_G}{C_0 - C}$$

Equation 9: Practical approach for Langmuir Isotherm set up

V is the volume of the protein solution, C is the expected protein concentration in the supernatant, V_G is the resin volume applied. K_a and q_{max} are estimations based on experimental results. The practical approach is simple by adding a defined volume of protein solution with known concentration to a defined resin volume in a test tube. Typically the test tube is incubated for 24 h on a rotor.

1.2.8 Adsorption kinetics – mass transfer in porous media

The transport of a protein into a porous particle starts with the external mass transfer, which is the transport of a solute from the surrounding fluid phase to the external surface of the particle. The driving force is the concentration difference across the boundary layer and is represented as the film mass transfer coefficient k_f (cm/s) which is depended on particle size, fluid viscosity and fluid velocity. General correlations for bed-packed adsorptions are expressed in terms of dimensionless Reynold (Re), Sherwood (Sh) and Schmidt (Sc) numbers and is shown in Equation 10:

$$Sh = \frac{1.09}{\varepsilon}\, Re^{0.33} Sc^{0.33}$$

Equation 10: Correlations for bed- packed adsorption for film mass transfer

where $Sh = k_f d_p/D$, $Re = u d_p/v$ and $Sc = v/D$; d_p is the particle diameter, D is the diffusion coefficient in free solution (cm^2/s) u is the superficial velocity (cm/h) and v is the kinematic viscosity(cm^2/s).

The diffusional transport from the outer surface into the particle pores is determined by the concentration gradient and is expressed in terms of the effective pore diffusion coefficient D_e (cm^2/s). D_e is typically smaller than the diffusivity in free solution because of the variation of pore size- and shape. This is considered in the tortuosity т. A value of т = 4 is assumed to be valid in bioseperation processes. D_e is also affected by steric hindrance due to viscous drag forces and size exclusion effects. The steric hindrance parameter K_P (-) can be estimated by:

$$K_P = 0.865\,(1 - 2.1\,\lambda_m + 2.09\,\lambda_m^3 - 0.984\,\lambda_m^5)$$

Equation 11: Estimation of hindrance parameter

λ_m is the ratio of radius of gyration of the protein r_m (cm) and the pore radius r_{pore} (cm). When taking particle porosity ε_p (-) into account D_e can be estimated:

$$D_e = \varepsilon_p\, D = K_p\, \frac{\varepsilon_p D}{\tau}$$

Equation 12: Estimation of effective pore diffusion coefficient

For practical applications, the dynamic binding capacity DBC is the most relevant parameter which describes the capture efficiency at a certain breakthrough. The breakthrough is determined by the dimensionless effluent concentration C/C_0 and is performed until saturation.

Values of 5 or 10% breakthrough are used for comparative applications. The DBC can be used to determine the effective pore diffusion coefficient D_e by the constant pattern solution for film and pore diffusion. The following equations are used to fit experimental breakthrough curves to determine D_e:

$$\tau_1 = (\frac{ut}{L} - \varepsilon)\frac{C_0}{(1 - \varepsilon)q_0}$$

Equation 13: formula of dimensionless time

$$N = \frac{15(1 - \varepsilon)D_e L}{ur_p^2}$$

Equation 14: formula of number of transfer units

τ_1 is the dimensionless time and N the number of transfer units (-) for pore diffusion, t is the time (s), L is the column length (cm), ε is the void fraction (-) and r_p is the radius of the particle (cm). For 10% breakthrough, the dimensionless time is:

$$\tau_1 = 1 - \frac{1.03}{N}$$

Equation 15: dimensionless time at 10% breakthrough

By plotting DBC/static capacity over N, D_e can be derived by curve fitting. One major advantage of using breakthrough curves to determine mass transfer kinetics is the operation in the column. Therefore, results can be directly used for scale up. One disadvantage is the necessity of high amount of protein solution for the experimental work.

Another method to investigate mass transfer kinetics is the use of a batch adsorption. In this method a defined resin volume is reacted with a protein solution in stirred vessel. At defined time intervals, samples are drawn and the protein concentration is measured. By plotting protein adsorption against time, it is possible to determine mass transfer rates. Important parameters to consider are the volume of added resin and the amount of protein solution which should be applied at a sufficiently high concentration so that a total protein adsorption is avoided [45][5].

1.3 Methods for Detection

1.3.1 GFP Quantification

Many biomolecules are fluorescent or can be labelled with fluorescent molecules, making fluorescence a widely used tool in analytical and imaging methods. Photons of a given wavelength are absorbed by the fluorophore and excite some of its electrons. The system remains in this excited state for only a few nanoseconds and then relaxes into its ground state. When returning from the excited state to the ground state, the electrons may emit photons. This is known as fluorescent emission. The wavelength of the absorbed photon is always shorter than that of the emitted photon, which means, that the energy of the emitted light is lower than that of the absorbed one. This phenomenon is called the Stok`s shift.

The relationship between wavelength λ, frequency v and energy E are shown in Equation 16 and Equation 17.

$$\lambda = \frac{c}{v}$$

Equation 16: wavelength depending on speed of light and frequency

$$E = hv$$

Equation 17: Energy calculation

λ is the wavelength in nm, v the frequency in 1/s, c is the speed of light with $3 * 10^9$ m/s, h is the Planck constant with $6.63 * 10^{-34}$ Js [46]

The fluorescence properties of GFP can be used to determine its concentration. Therefore a standard calibration curve is used to determine the GFP concentration in solution.

1.3.2 Endotoxin Quantification

Components existing in the blood of horseshoe crabs can form a clot when exposed to Endotoxin. The reaction cascade which is shown Figure 10 starts with the activation of Factor C, which is a serine protease precursor in the presence of Endotoxin. Factor C activates Factor B, which is also a serine protease precursor and a proclotting enzyme. The activated clotting enzyme converts soluble proteins (coagulogen) to an insoluble complex (coagulin) by cleaving the *L. polyphemus* coagulogen at the Arg- Lys and Arg- Gly linkage resulting in the release of peptide C and formation of the characteristic gel. The proteolytic activity of the activated clotting enzyme is also present against specific chromogenic substrates hydrolysing the terminal Gly-Arg-p-nitroaniline in the following reaction:

Substrate + Enzyme + H_2O → Peptide + p-Nitroaniline. p- Nitroaniline is distinctively yellow. The intensity of the yellow colour can be used to determine the Endotoxin on a quantitative level. One disadvantage of the LAL – reagents is, that they react not only with the endotoxin but also $(1 \rightarrow 3)$-β-D-glucan, a fungal cell wall component, since the Factor G pathway can be activated with these reagents.

A compromising alternative to the LAL test is the use of a recombinant Factor C also shown in Figure 10: Reaction cascade - LAL and Recombinant Factor CDue to the use of the recombinant Factor C, animal based sources can be reduced and the Factor G cascade can be avoided. [47][48] (Figure 10:changed from [49])
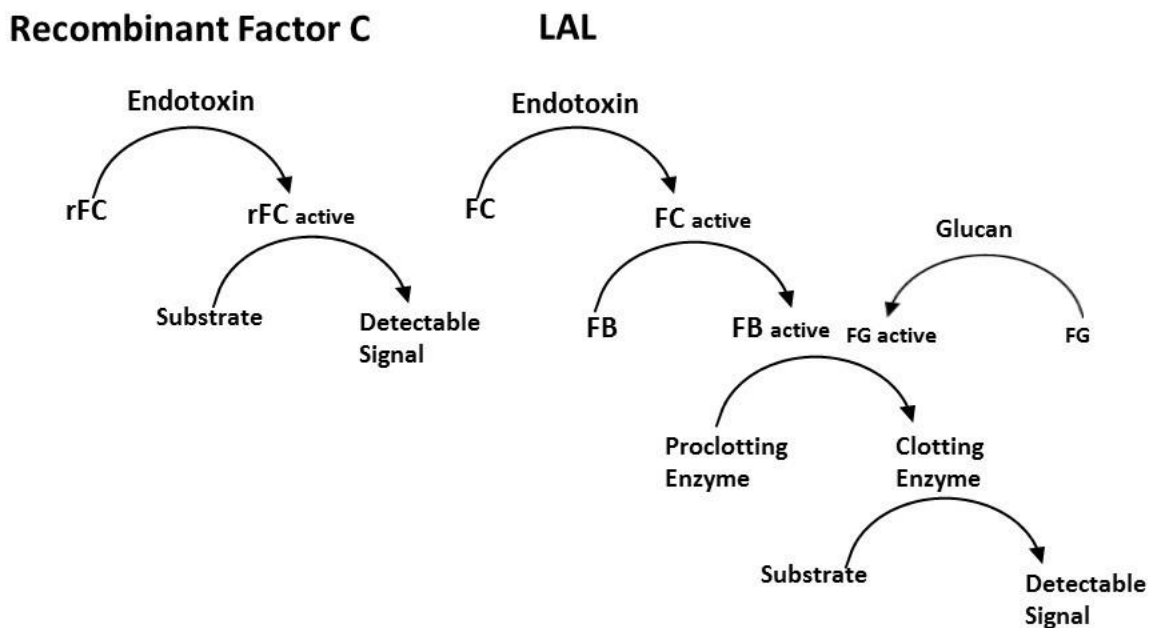

Figure 10: Reaction cascade - LAL and Recombinant Factor C

1.3.3 DNA Quantification

The most common method for the quantification of DNA is to measure the absorption in the UV region at 260 nm. Since proteins also absorb at this wavelength, this method is not preferable, when measuring the DNA levels in protein solutions. An alternative method is the use of the fluorochrome Hoechst 33258. Hoechst 33258 is a benzimidazole dye that binds to the minor groove of double stranded DNA with a preference for adenine and thymine-rich sequences. DNA binding leads to shift of the fluorescent output which can be measured by an excitation wavelength of 360 nm and an emission wavelength of 460 nm. Hoechst binds to double-stranded DNA and also to single- stranded DNA but with less efficiency. It does not bind to small oligomers. The unknown DNA samples are measured with against a standard curve generated with calf-thymus DNA, which is double-stranded and has an AT content of 58%.[50]

1.3.4 Nephelometry

The principle of nephelometry is that light passing through a liquid medium may be scattered and absorbed by inhomogeneity's in the light path, especially suspended particles. Scattering occurs when a particle interacts with incident light by absorbing the light energy. Comparison of the intensity of light scattered by the sample with the intensity of light scattered by a standard reference suspension gives information turbidity of the sample. The higher the intensity of scattered light, the higher the turbidity. The intensity of the scattered light is expressed as Nephelometric turbidity unit – NTU. [51][52]

1.3.5 SDS – PAGE

The Sodium Dodecyl Sulphate Polyacrylamide Gel Electrophoresis is a method to evaluate the purity of a protein solution by size separation in an electric field. The anionic detergents SDS denature the proteins by disturbing the non-covalent forces. Furthermore the SDS charges the proteins negatively. The amount of SDS bound to the proteins is proportional to the molecular size. The denatured protein molecules are then loaded onto the polyacrylamide gel and an electric field is applied. The negatively charged proteins migrate to the anode. Smaller proteins migrate faster than big proteins, which are hindered by the polyacrylamide gel. By using a standard protein solution, the size of the proteins can be determined.[53]

2. Material and Methods

2.1 Host strain

Escherichia coli host strain HMS174(DE3), carrying the plasmid pet11a_GFP_mut3.1

2.2 High Pressure Homogenisation

2.2.1 Equipment

- 2 Stage Homogeniser - Panda PLUS - (GEA Niro Soavi, Düsseldorf, Germany)
- 2 Stage Homogeniser Panda NS 1001 L2K – (GEA Niro Soavi, , Düsseldorf, Germany)

2.2.2 Material

- Chemicals from Merck, Darmstadt, Germany
- Homogenisation buffer 1: 50 mM Tris, 100 mM NaCl pH 8
- Homogenisation buffer 1: 50 mM Tris, 50 mM NaCl pH 8
- Flushing solution: dH_2O
- Cleaning solution: 0.1 M NaOH in dH_2O
- Storing solution: 20% Ethanol in dH_2OW

2.2.3 Method

Prior to high pressure homogenisation, *E. coli* cells were resuspended with the homogenisation buffer to a final cell dry mass concentration of 25 g/L. The cell suspension was stirred until a homogenous suspension was formed and no cell clumps were visible. Afterwards the homogenizer which was stored in 20% Ethanol was turned on and flushed with dH_2O without pressure. The next step was a flow test under pressure with 700 bar in the first stage and 70 bar in the second stage. A flow of approx. 200 mL/min has to be achieved. If the flow test was in the acceptable range, the homogenisation of the cell suspension was started. Table 1 shows the applied pressures and the number of passages used for this experiment.

Table 1: Applied pressures and number of passages for homogenisation trials

Number of Passages	1. Stage	2. Stage
1	400	40
2	400	40
1	500	50
2	500	50
1	600	60
2	600	60
1	700	70
2	700	70

2.3 Polyethyleneimine flocculation

2.3.1 Equipment

- Vortexer - IKA VORTEX GENIUS 3 (Merck, Darmstadt, Germany)

2.3.2 Material

- 10 kDa branched Polyethyleneimine (Polyscience, Warrington, USA)

2.3.3 Method:

The 10 kDa branched Polyethyleneimine (PEI) was diluted with dH_2O to a 10% (w/v) solution. In the first experiment the 10% PEI solution was added to 25 mL of the *E.coli* homogenate (500/50 bar 1 passage) with a CDM of 25 g/L to a final concentration shown in Table 2:

Table 2: PEI added to E.coli homogenate - 25 mL scale

Final PEI concentration [% w/v]	Added PEI [µL]
0.075	187.5
0.1	250
0.125	312.5
0.15	375
0.175	437.5
0.2	500
0.25	625
0.3	750
0.4	1000
0.45	1125
0.5	1250

Then the samples were vortexed and the PEI flocculation was evaluated after centrifugation with 4000 g for 30 min in terms of turbidity, GFP-, DNA- and endotoxin concentration. An untreated homogenate was used as reference. In the next step the scale was elevated to 250 mL homogenate with a final CDM of 25 g/L. The PEI was added according to Table 3. The samples were evaluated after centrifugation shown section 2.5 and after ultra- and diafiltration shown in section 2.6 in terms of turbidity, average permeate flow and GFP concentration. For the untreated homogenate, also the DNA- and endotoxin levels were measured.

Table 3: PEI added to E.coli homogenate - 250 mL scale

Final PEI concentration [% w/v]	Added PEI [mL]
0.2	5
0.3	7.5

2.4 Polyethyleneimine flocculation in combination with heat-treatment

2.4.1 Equipement:

- Watherbath -Lauda AQUAline AL (LAUDA-Brinkmann, LP, Delran, USA)
- Vortexer - IKA VORTEX GENIUS 3 (Merck, Darmstadt, Germany)

2.4.2 Material:

- 10 kDa branched Polyethyleneimine (Polyscience, Warrington, USA)

2.4.3 Method:

The water bath was filled with dH_2O and pre-warmed to 50 °C. The PEI solution was prepared in the same way as shown in 2.3.3 and the PEI concentration was added according to Table 2. An untreated homogenate was used as reference sample. The PEI- treated samples and the reference sample were vortexed, placed into the water bath and incubated for 3h. In the next step the scale was elevated to 250 mL homogenate with a final CDM of 25 g/L. The PEI was added according to Table 3 in section 2.3.3. The samples were evaluated after centrifugation shown in section 2.5 and after ultra- and diafiltration shown in section 2.6 in terms of turbidity, average permeate flow and GFP concentration. For the heat-treated homogenate without PEI also DNA- and endotoxin levels are measured.

2.5 Cell debris removal

2.5.1 Equipment

- Centrifuge – HERAEUS MULTIFUGE X3 FR Centrifuge with a Swing- out bucket rotor. (Nr. 75003607 max. 4700 rpm) - Thermo Scientific
- Centrifuge - Avanti JXN-26 Centrifuge with a fixed angle rotor (JLA-10.500 max 10000 rpm) and centrifuge buckets - BECKMAN COULTER
- Lab balance- ENTRIS5201-1S (max 5200 d=0.1) - Sartorius

2.5.2 Method:

The samples with a volume of 25 mL shown in section 2.3 and 2.4 were balanced to a weight difference of 0.1 g and centrifuged with 4000 g for 30 minutes at 4 °C with the swing out centrifuge. The samples with a volume of 250 mL shown in section 2.3 and 2.4 were balanced to a weight difference of 0.1 g in the centrifuge bucket and centrifuged with 10,000 rpm for 1 hour at 4 °C with the fixed angle centrifuge. After centrifugation, the supernatants of the samples were transferred to new flasks. The cell debris pellets were discarded.

2.6 Ultra- and Diafiltration

2.6.1 Equipment:

- Ultra-and Difiltration system -MILLIPORE Labscale^{TM} TFF System (Merck, Darmstadt, Germany)

- Membrane Filter - MILLIPORE PELLICON XL FILTER – 50 cm^2 regenerated cellulose membrane with a cut off of 10 kDa (Merck, Darmstadt, Germany)

2.6.2 Material:

- Chemicals from Merck, Darmstadt, Germany

- Diafiltration buffer: 10 mM Tris/HCl pH 7.5

- Cleaning solution: 0.1 M NaOH

- Storage solution: 0.05 M NaOH

2.6.3 Method:

Prior to filtration, the membrane was connected to the TFF system. Preconditioning, cleaning and storage of the system was performed according to the PELLICON XL Operation Instructions. For the ultrafiltration process the supernatant was transferred into the filtration tank, the pump was started and the transmembrane pressure was adjusted to 2.5 bar by the feed pressure and retentate back pressure. The supernatant was concentrated to a final GFP concentration of approx.11 mg/mL. This was typically achieved by a concentration factor of 2.5-3. The ultrafiltration process was evaluated by measuring GFP-, DNA -and endotoxin concentration and the turbidity of the ultrafiltration retentate. After ultrafiltration, a reservoir with diafiltration buffer was connected to the TFF System. The system was made airtight by using a lid for the filtration tank and a syringe for the open vent. The syringe was also used for the application of the diafiltration buffer to the filtration tank. Afterwards the pump was started and the transmembrane pressure was adjusted to 2.5 bar. The diafiltration process was performed until 5 volume changes have been made. This was evaluated by measuring of the permeate volume. After the diafiltration process, the GFP-, DNA- and endotoxin concentration and the turbidity were measured. A final GFP concentration of approx. 10 mg/mL had to be achieved.

2.7 Adsorption Isotherms:

2.7.1 Equipment:

- Rotator -Stuart rotator SB3
- Centrifuge- Eppendorf Centrifuge 5415 R
- Micro Centrifuge- Carl Roth

2.7.2 Material:

- CaptoQ resin – (GE Healthcare, Chicago, USA)
- Equillibration buffer: 10 mM Tris/HCl pH 7.5

2.7.3 Method:

The CaptoQ resin was stored in 20% ethanol and had to be washed 5 times with the equilibration buffer. This was done by transferring 2 mL of the resin into an Eppendorf tube. The tube was spinned down with the micro centrifuge, afterwards the supernatant was discarded. The resin was filled up with fresh equilibration buffer and re-suspended to a slurry. In the final step the slurry was adjusted to a punctilious ratio of 50% resin and 50% equilibration buffer. From this slurry, defined volumes were transferred to 2 mL Eppendorf tubes and a defined volume of protein solution was added to the slurry volume. In the next step the samples were mixed and incubated for 24 hours on the overhead rotator. After incubation, the samples were centrifuged in the Eppendorf centrifuge for 30 min with 9000 rpm at 4 °C. After centrifugation, the supernatants were measured in terms of GFP-, DNA- and endotoxin concentration. Table 4 shows the setup for the heat-treated homogenate (HP), the heat-and PEI treated homogenate (HP+PEI) and the homogenate after PEI treatment (HO+PEI). All of these samples were ultra- and diafiltrated. Table 5 shows the setup of the heat and PEI treated homogenates and the homogenates after PEI treatment. The samples were ultrafiltrated and diluted 1:2 with dH_2O. Table 6 shows the setup of the homogenate after ultra- and diafiltration. The equilibrium binding capacity EBC at a certain resin volume was calculated by the difference between initial concentration of the protein solution and the concentration of the protein solution at this resin volume after incubation. The EBC of DNA and endotoxin was calculated by the use of the mass balance, which takes into account the volumes of the slurry and the sample.

Table 4: setup for adsorption isotherms: diafiltrated HP, HP+PEI and HO+PEI

V Slurry [mL]	V resin [mL]	V sample[mL]	V corr. [mL]
0.020	0.010	1.5	1.520
0.040	0.020	1.5	1.540
0.060	0.030	1.5	1.560
0.081	0.040	1.5	1.581
0.101	0.051	1.5	1.601
0.122	0.061	1.5	1.622
0.142	0.071	1.5	1.642
0.164	0.082	1.5	1.664
0.189	0.095	1.5	1.689
0.209	0.105	1.5	1.709

Table 5: setup for adsorption isotherms for ultrafiltrated: HP+PEI, HO+PEI

V slurry [mL]	V resin [mL]	V sample [mL]	V corr. [mL]
0.8	0.4	1	1.8
0.4	0.2	1.5	1.9
0.3	0.15	1.5	1.8
0.2	0.1	1.5	1.7
0.1	0.05	1.5	1.6
0.05	0.025	1.5	1.55

Table 6: setup for adsorption isotherms: diafiltrated HO

V slurry [mL]	V resin [mL]	V sample [mL]	V corr [mL]
0.020	0.010	1.5	1.520
0.060	0.030	1.5	1.560
0.101	0.051	1.5	1.601
0.142	0.071	1.5	1.642
0.209	0.105	1.5	1.709

2.8   Batch Adsorption

2.8.1 Equipment:

- Magnetic Stirrer IKA RH basic 2

2.8.2 Material:

- Capto Q resin (GE Healthcare, Chicago, USA)
- Millipore Millex-GV filter 0.22 µm
- Equillibration buffer: 10 mM Tris/HCl pH 7.5 (

2.8.3 Method:

Prior to batch adsorption experiment, a 50% resin of CaptoQ and 50% of equilibration buffer was made. This was performed in the same way as described in section 2.7. The general experimental approach is to combine a defined slurry volume with a defined sample volume containing a known protein concentration. This was performed with a magnetic stirrer at low speed. At certain time-points a sample was drawn by using a syringe. The sample was then

immediately pressed through a filter to stop adsorption. The filtrate was measured for the GFP-DNA- and endotoxin concentration. The binding capacity at a certain time point was calculated by the difference between initial concentration of the protein solution and the concentration of the protein solution at this time point, assuming a constant volume of protein solution per resin ratio. Three different starting solutions were used: a diafiltrated homogenate (HO), a diafiltrated heat-treated homogenate (HP) and a diafiltrated heat-treated homogenate which had been treated with 0.2% PEI w/v (HP+PEI). The volumes of sample and resins, i.e. slurry as well as time points for sample suction are shown in Table 7. The setup was estimated according to the results of the adsorption isotherms with a starting GFP concentration of 10 mg/mL for all sample where approx. 50% of the GFP was adsorbed onto the resin.

Table 7: Setup for batch adsorption

Sample	Vsample [mL]	Vslurry [mL]	Vresin [mL]	time point of sample [min]
HO	20	1.5	0.75	0.5, 1, 2, 15, 30, 60, 120, 360, 490,620, 690
HP	20	1	0.5	0.5, 1, 5, 15, 30, 60,120,180,240, 300, 470, 690, 1440
HP+PEI	16	0.4	0.2	0.5, 1, 5, 15, 30, 60, 240, 1200, 1400

2.9   Anion Exchange Chromatography – Break-through curves

2.9.1 Equipment

- Äkta Explorer
- Tricorn5 column (h: 5.4 cm, d: 0.5 cm, v: 1.06)

2.9.2 Material

- Capto Q resin - GE Healthcare, Chicago, USA
- Equillibration buffer: 10 mM Tris/HCl pH 7.5
- Elution buffer: 10 mM Tris 1 M NaCl
- Regeneration solution: 0.1 M NaOH
- Acetone

2.9.3 Method:

A one mL column of CaptoQ resin was packed according to the manufactureres instruction and packing performance evaluated using an acetone pulse experiment. The evaluation is shown in Figure 42 in section 9. For the experiment, three different starting solutions are used: a diafiltrated homogenate (HO), a diafiltrated heat-treated homogenate (HP) and a diafiltrated heat-treated homogenate which had been treated with 0.2% PEI w/v (HP+PEI). The samples were loaded with 2 different residence times in a scout program and one mL samples were

collected until elution with 100% elution buffer via automated fractionation. Table 8 shows the setup for the break-through experiment based on the measured GFP concentrations after diafiltration and was estimated according to the results of the binding capacity of the adsorption isotherms.

Table 8: setup for breakthrough experiments

Sample	Residence time [min]	Volumentric flow [mL/min]	Proteinload [mgGFP/column]
HP+PEI	1.5	0.71	318
HP+PEI	9	0.12	318
HP	1.5	0.71	265
HP	9	0.12	265
HO	1.5	0.71	212
HO	9	0.12	212

Before loading the samples onto the column, the column was equilibrated with 4 column volumes CV using equilibration buffer. Afterwards, the samples were loaded according to Table 8. Loading of the samples was completed by addition of a loading of 2 CV further sample and 2 CV of equilibration buffer were applied to wash out unbound sample. The GFP was eluted using a step gradient with 5 CVs of 30% elution buffer and afterwards 5 CVs of 100% elution buffer. The column was regenerated with 2 CVs of 0.1 M NaOH, washed with 2 CVs of elution buffer and re- equilibrated with 5 CVs of equilibration buffer. The breakthrough-curves were evaluated using the constant pattern solution for film- and pore diffusion, which is described in section 1.2.8. For the diafiltrated homogenate and the diafiltrated heat-treated homogenate, DNA and endotoxin measurements were performed. DNA concentration was measured in every single sample, which was collected via auto- fractionation. For endotoxin measurement, pools of the collected samples were made. For the diafiltrated homogenate the first pool consist of the first 7 mL collected, the second pool consists of the next 5 mL, the third pool of the next 3 mL and the fourth pool of the last 3 mL in the breakthrough. Furthermore, the eluate at 30% elution buffer- and the eluate at 100% elution buffer were pooled separately. For the diaflitrated heat-treated homogenate also 4 pools were made from the breakthrough curve. The first pool consists of the first 11 mL, the second of the next 5 mL, the third and the fourth pool of the respectively following 5 mL. Also the eluate at 30%- and 100% elution buffer were pooled separately.

2.10   DNA Quantification

2.10.1 Equipment

- Tecan InfiniteM200 Pro

2.10.2 Material

- DNA Quantification kit - BIO RAD DNA Quantitation Kit (Catalog Number 170-2480)
- 96 well plates -Thermo Scientific Nunclon 96 Flat Bottom Black Polystyrol LumiNunc FluoroNunc

2.10.3 Method

DNA quantification was performed according to the instruction manual of the DNA Quantitation Kit for a Hoechst 33258 concentration of 2 µg/mL and a volume of 200 µL in the micro titer plate. Afterwards 2-5 µL of sample was added to the Hoechst dye. For each measurement a standard calibration curve was measured with the samples of interest. Table 9 shows the parameters for DNA measurement in the Tecan reader. Figure 11 shows an example of a DNA standard calibration curve.

Table 9: parameters for DNA Quantitation in the Tecan Reader

| Mode				Fluorescence Top Reading		
Excitation Wavelength				355	nm	
Emission Wavelength				460	nm	
Excitation Bandwidth				9	nm	
Emission Bandwidth				20	nm	
Gain				95	Manual	
Number of Flashes				25		
Integration Time				20	µs	
Lag Time				0	µs	
Settle Time				0	ms	
Z-Position (Manual)				20000	µm	
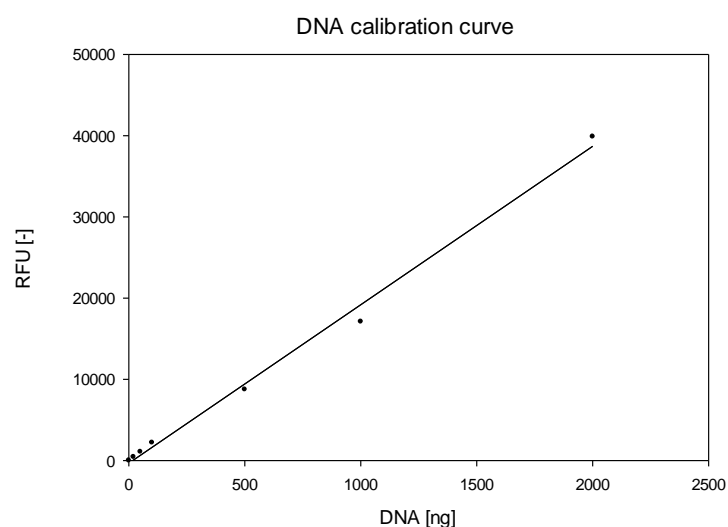
Figure 11: DNA calibration curve

In this example, the linear regression analysis led to the equation: y = 19.511x - 318.09 with an r^2 of 0.9945 and is displayed as ng DNA. To determine the DNA concentration in mg/ml, the linear regression was divided by the applied sample volume.

2.11 GFP measurement

2.11.1 Equipment

- Tecan InfiniteM200 Pro

2.11.2 Material

- DNA Quantification kit - BIO RAD DNA Quantitation Kit (Catalog Number 170-2480)
- Thermo Scientific Nunclon 96 Flat Bottom Black Polystyrol LumiNunc FluoroNunc

2.11.3 Method:

GFP was quantified by measuring the fluorescence signal of the sample which has to be in the linear range of the GFP calibration curve shown in Figure 12. For measurement, 100 µL of sample or diluted sample was pipetted into the microtiter plate. The calibration curve was taken from [30]. The parameters for the measurement in the Tecan reader are shown in Table 10.

Table 10: parameters for GFP Quantification

| Mode			Fluorescence Top Reading		
Excitation Wavelength			485	nm	
Emission Wavelength			520	nm	
Excitation Bandwidth			9	nm	
Emission Bandwidth			20	nm	
Gain			53	Manual	
Number of Flashes			40		
Integration Time			20	µs	
Lag Time			0	µs	
Settle Time			0	ms	
Z-Position (Manual)			18811	µm	
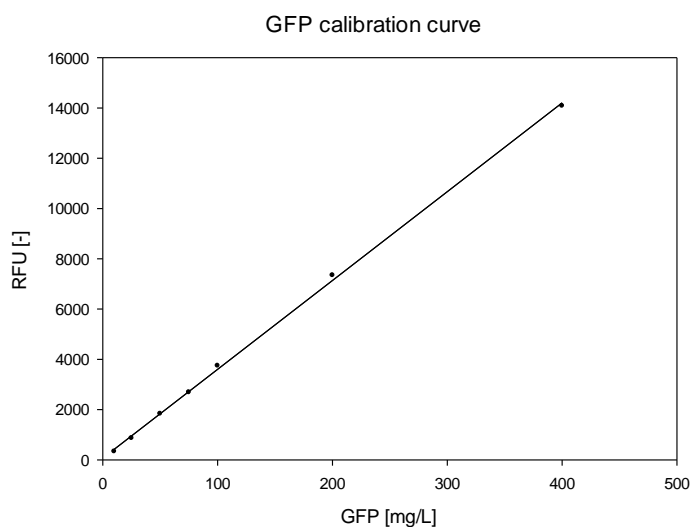
Figure 12: GFP calibration curve

In this example, the linear regression which was: $y = 35.341x + 67.923$ with a $R^2 = 0.9993$ was used to calculate the GFP concentration of the samples of interest.

2.12 Endotoxin measurement

2.12.1 Equipment

- Tecan InfiniteM200 Pro

2.12.2 Material - LAL

- Endotoxin assay - Lonza LAL QCL-100™
- Greiner 96 well flat transparent Polystyrol (sterile)
- G Bioscience Endotoxin free Water (Catalog-Nr 786-670)

2.12.3 Method - LAL

Endotoxin quantification was performed according to the instruction manual of Lonza LAL QCL-100™ assay. For each measurement, a standard calibration curve was performed in dublicates. The samples of interest were measured at a dilution that the signal obtained was within the calibration curve. The dilutions were made with Endotoxin free water in sterile 12 mL Greiner tubes within the linear range of the calibration curve. The measurement was performed in the Tecan reader at a wavelength of 405 nm. Figure 13 shows an example of a generated calibration curve.
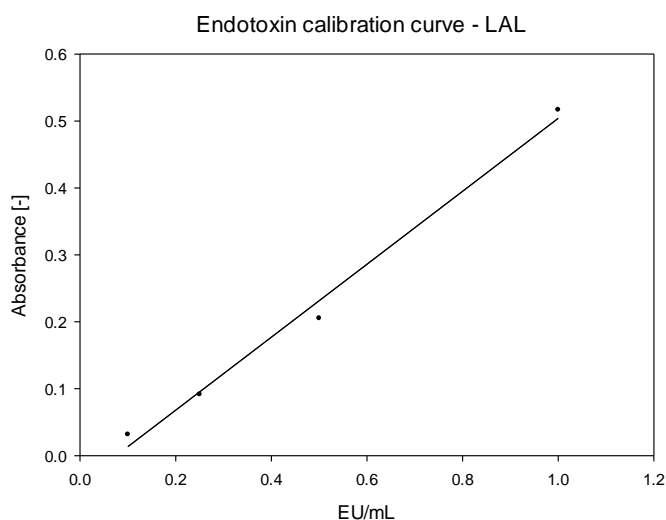

Figure 13: Endotoxin calibration curve - LAL

The linear regression which is: $y = 0.5451x - 0.041$ with a $R^2 = 0.9914$ was used to calculate the endotoxin concentration of the samples of interest.

2.12.4 Material -Recombinant Factor C Endotoxin Detection Assay

- Endotoxin assay- Hyglos GmbH EndoZyme^R II

- 96 well plates- Thermo Scientific Nunclon 96 Flat Bottom Black Polystyrol LumiNunc FluoroNunc

- Endotoxin free Water - G Bioscience (Catalog-Nr 786-670)

2.12.5 Method: Recombinant Factor C Endotoxin Detection Assay

Endotoxin quantification was performed according to the instruction manual of EndoZyme II REF 890030 with the adjustment that two additional calibration points were performed at 1 EU/mL and 0.1 EU/mL. The standard calibration curve was performed in dublicates for every measurement. The samples of interest were measured at a dilution that the signal obtained is within the calibration curve. The dilution were made with Endotoxin free water in sterile 12 mL Greiner tubes within the linear range of the calibration curve. Table 11 shows the parameters for the Endotoxin quantification. Figure 14 shows an example of a measured calibration curve.

Table 11: parameters for Endotoxin Quantification – Recombinant Factor C

| Mode			Fluorescence Top Reading		
Excitation Wavelength			380	nm	
Emission Wavelength			445	nm	
Excitation Bandwidth			9	nm	
Emission Bandwidth			20	nm	
Gain			100	Manual	
Number of Flashes			40		
Integration Time			20	µs	
Lag Time			0	µs	
Settle Time			0	ms	
Z-Position (Manual)			18811	µm	
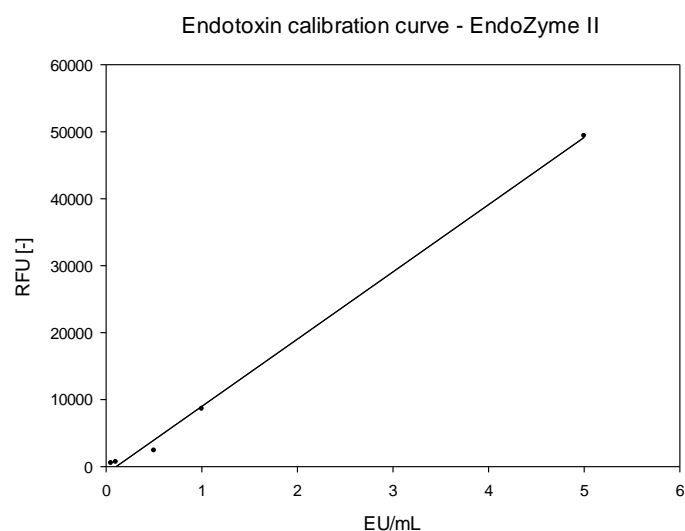
Figure 14: Endotoxin calibration curve – Endozyme II

The linear regression which was: y = 10000.07x - 1041 with a R² = 0.9975 was used to calculate the endotoxin concentration of the samples of interest.

2.13 Nephelometry – Turbidity measurement

2.13.1 Equipment

- Nephelometer -Hach-Lange 2100Q

2.13.2 Material

- 800 NTU Hach STABLCAL Formazin
- 10 NTU Hach STABLCAL Formazin

2.13.3 Method

For turbidity measurement, the nephelometer was calibrated using a 10 NTU and a 800 NTU standard. Afterwards the samples of interest were transferred into a cuvette and measured. Approx. 12- 15 mL of sample is necessary for each measurement.

2.14 SDS-PAGE

2.14.1 Equipment

- Invitrogen XCell Sure Lock™
- Invitrogen Novex Mini-Cell
- Pharmacia Biotech Electrophoresis Power Supply EPS600
- BIO-RAD Mini-Protean® Tetra-System
- BIO-RAD Power Pac Basic
- Eppendorf™ Thermomixer™ R

2.14.2 Material

- NuPAGE 4-12% Bis Tris Gel
- Dilution buffer: 10 mM Tris pH 7.5
- NuPAGE reducing agent
- NuPAGE LDS sample buffer
- Fixing solution: 500 mL 96% ethanol, 100 mL glacial acetic acid
- Staining solution: 200 mL 96% ethanol, 50 mL glacial acetic acid, 1 g Coomassi Blue R250
- Destaining solution: 250 mL 96% ethanol, 80 mL glacial acetic acid
- Running buffer: MES SDS running buffer
- Mark12 standard

2.14.3 Method

For the SDS-PAGE the samples 13 µL of sample was incubated with 5 µL of sample buffer and 2 µL of reducing agent for 10 min on the thermomixer at 70 °C with 600 rpm. Before incubation, the samples were diluted to a final protein content of 15 µg. Afterwards the

NuPAGE gel was washed with water and placed into the Mini-Cell chamber. The chamber was filled with running buffer and the protein solutions were loaded onto the gel. A Mark12 was used as standard. Then the electrophoresis was started at 200 V and 400 mA and stopped after approx. 45 min. Afterwards the gel was flushed with water and incubated with the fixing solution for 30 min on a shaker. In the next step, the fixing solution was discarded and the gel was incubated for 30 min with the staining solution. After discarding the fixing solution, the gel was incubated with the destaining solution until the gel is sufficiently destained. Finally the gel was scanned and evaluated.

3. Results and Discussion

3.1 Homogenisation experiments

Aim of homogenisation experiments was to investigate if different applied pressures and number of passages have influence on DNA and Endotoxins contents. They can also be regarded as follow up experiments to the one of Zartler [30], in which it was shown that a higher applied pressure leads to a higher protein release and that more passages lead to a reduction of particle size, which influences the centrifugation- and filtration performance. They can also be seen as follow up experiments to the one of Fink [39], where it was shown that more passages lead to a decrease of the viscosity of the solution due to DNA fragmentation. The degree of protein release was evaluated by GFP quantification with the assumption that a homogenisation with an applied pressure of 700 bar in the first stage- and 70 bar in the second stage effects 100% protein release after two passages. Table 12 gives an overview of the results of the homogenization experiments. In this table the second stage is always denoted first, since the pressure at the second stage is applied first, due to practical considerations.

Table 12: Results of homogenisation experiments

Sample	GFP [mg/mL]	GFP release [%]	DNA [mg/mL]	Endotoxin [EU/mL]
40/400 1. Passage	4.16	85.0	0.757	833,543
40/400 2. Passage	4.63	94.6	0.808	871,561
50/500 1. Passage	4.28	87.6	0.776	890,569
50/500 2. Passage	4.67	95.6	0.845	987,989
60/600 1. Passage	4.82	98.5	0.653	828,791
60/600 2. Passage	4.70	96.2	0.753	1,027,194
70/700 1. Passage	4.56	93.2	0.709	1,121,050
70/700 2. Passage	4.89	100.0	0.808	1,169,760

3.1.1 Endotoxin levels in homogenates

Application of different pressures and the performance of 1 and 2 passages revealed a clear trend for the endotoxin concentrations as shown in Figure 15.
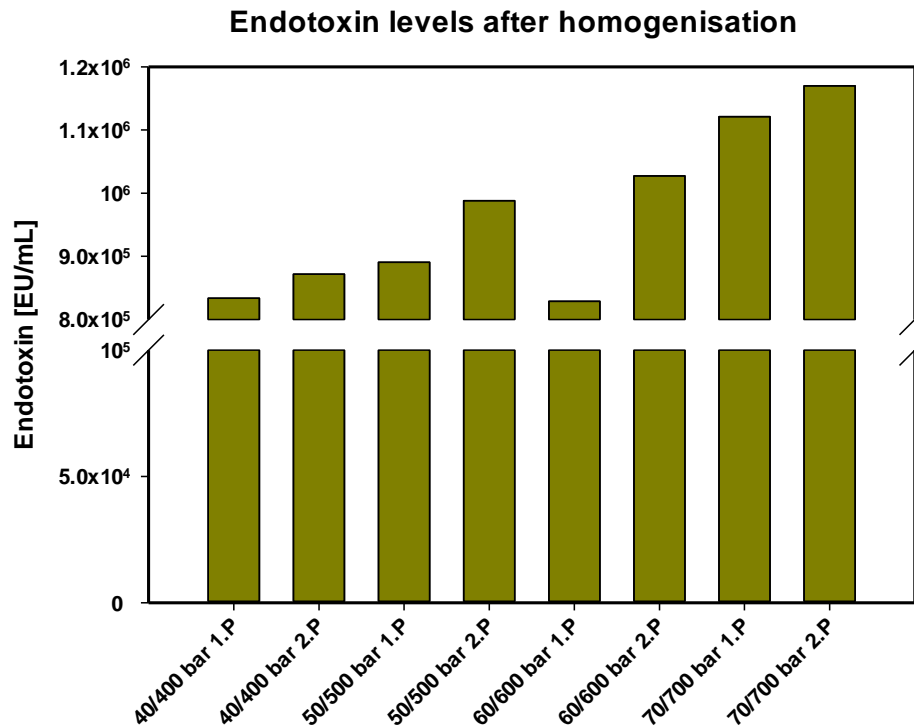

Figure 15: Endotoxin concentrations after homogenisation experiments at 25 g/L CDM

The highest release of Endotoxin was observed at 70/700 bar and 2 passages with approx. 1.2 million EU/mL. For these conditions it is also assumed, that a 100% protein release is achieved. However, under these conditions the highest degree of cell disruption i.e. disruption of the *E. coli* cell membrane was observed. As mentioned before, endotoxins are very stable molecules, which are part of the outer membrane *E. coli* cells. Therefore it is reasonable, that with the highest degree of disruption also the most endotoxins are released into the supernatant. With decreasing pressure applied, also the release of endotoxin decreased. Considering the applied pressures after the first passage, the highest endotoxin release was observed at 70/700 bar with approx. 1,100,000 EU/mL followed by 50/500 bar with 890,000 EU/mL, and 830,000 EU/mL at 40/400 bar. The endotoxin release at 60/600 bar was the lowest with also approx. 830,000 EU/mL. This result was surprising since it does not fit the trend of the other results where an increase of pressure leads to an increase of endotoxin release. It is suspected, that this result was either just a measurement error due the high dilutions, which are necessary for endotoxin quantification or was caused by pressure fluctuations during the homogenization process which led to uncontrolled conditions. In comparison to the DNA release at these conditions which is shown in the next section it is

more likely due to pressure fluctuations. For the second passage, the trend was also the same. The lowest Endotoxin release was observed at 40/400 bar with 870,000 EU/mL, followed by 50/500 bar with 990,000 EU/mL, 1,000,000 EU/mL at 60/600 bar and the highest Endotoxin release at 70/700 bar which has already been shown above. Also when comparing the two passages at an applied pressure a clear trend was obtained. The Endotoxin level always increased after the second passage for every applied pressure. At 40/400 bar the endotoxin led to an additional endotoxin release of 5% after the second passage. At 50/500 bar by 11%, at 60/600 bar by 12.5% and at 70/700 by 5%. This is a reasonable result since cell disruption is higher after the second passage.

3.1.2 DNA levels in homogenates

DNA release by HPH at different pressure levels and number of passages is shown in Figure 16.
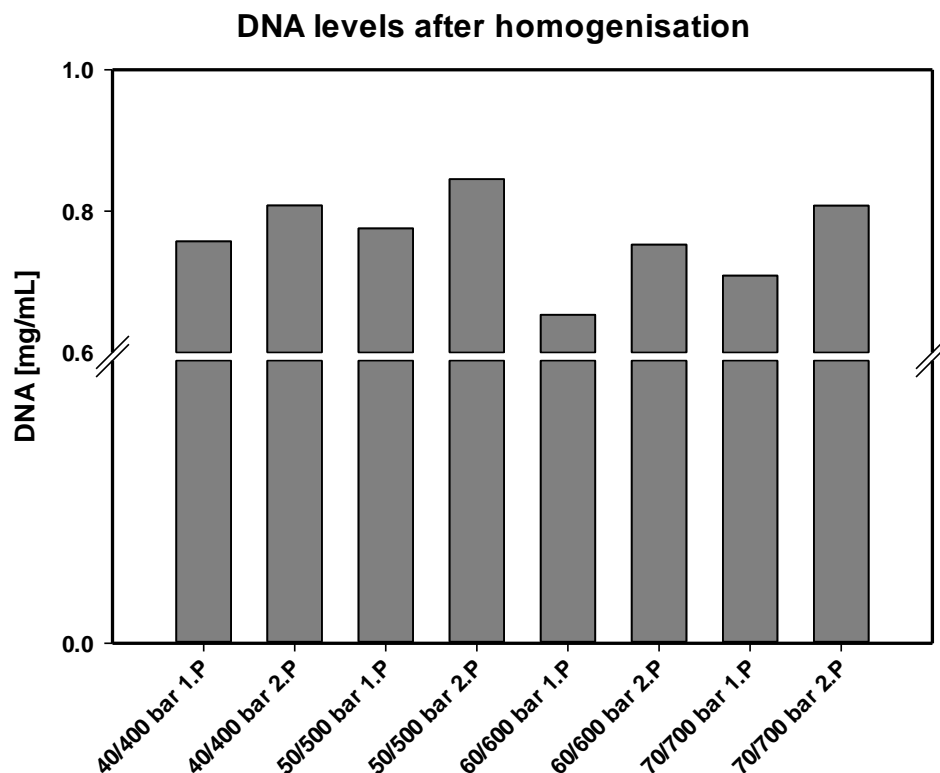
Figure 16: DNA concentrations after homogenisation experiments

Comparing the results of the first and second passage the trend is similar to the results of the endotoxin levels in terms of higher release of DNA upon the second passage. In contrast, higher pressure apparently did not increase DNA release significantly. However, on one hand higher pressure and on the one hand more passages lead to enhanced DNA fragmentation. In turn, staining of smaller DNA fragments is less effective and very small DNA oligomers are not detected at all [50]. Consequently a full evaluation of DNA release dependent on operating

conditions was not possible with the applied analytical method. The lowest DNA concentration was measured after 60/600 bar after the first passage. As has been mentioned in the last section, pressure fluctuation could be possible reason for this unexpected result since DNA quantification does not need high sample dilution. Also the GFP release didn`t correlate with the trend, where the second highest protein released determined in the experiment with 98.5% protein release after the first passage and a decreasing protein release after the second passage with 96.2%.

3.2 PEI flocculation

3.2.1 PEI flocculation of homogenate and heat- treated homogenate - 25 mL scale

The separation of small debris, which are generated during HPH can reduce the centrifugation performance when considering Stoke`s law where the settling velocity in a gravitational- and accelerated centrifugal field is depended on the square of the particle diameter. The use of the cationic flocculant Polyethyleneimine can significantly increase the particle diameters of the cell debris after homogenisation by polymer bridging but can also precipitate soluble molecules like DNA and endotoxins. Aim of this investigation was to study the effect of different PEI concentrations on the efficiency of cell debris removal of a homogenate and also of a heat-treated homogenate. A comparative analysis was performed by turbidity measurement after centrifugation with 4000g for 30 min. Furthermore, the DNA- and endotoxin concentrations were measured after PEI treatment. Experiments were performed with an E. coli homogenate with a CDM of 25 g/L after 50/500 bar and one passage at a pH of 8. Since also GFP with a pI of 5.9 is negatively charged at this pH, it was investigated, if there is a product lost after PEI treatment. Table 13: shows the results of the homogenate, Table 14 shows the results of the heat-treated homogenate.

Table 13: Results of the homogenate after PEI treatment-25 g/L CDM

%PEI [w/v]	NTU [-]	DNA [mg/mL]	Endotoxin [EU/mL]	GFP [mg/mL]
0	507	1.06	7,494,726	4.76
0.075	400	0.16		5.01
0.1	354	0.23	2,574,245	5.18
0.125	283	0.11		5.22
0.15	238	0.07	1,234,426	5.07
0.175	24	0.05		5.29
0.2	10	0.06	616	5.28
0.25	10	0.07		5.30
0.3	14	0.06	473	5.67
0.4	18	0.06	512	5.33
0.45	10	0.07		5.00
0.5	42	0.06	499	4.82

%PEI [w/v]	NTU [-]	DNA [mg/mL]	Endotoxin [EU/mL]	GFP [mg/mL]
0	148	0.10	2,579,162	4.76
0.075	118	0.08		4.76
0.1	110	0.07	1,250,333	4.86
0.125	106	0.07		5.03
0.15	91	0.06	737,268	5.25
0.175	27	0.04		4.95
0.2	19	0.04	1,097	5.17
0.25	12	0.05		5.29
0.3	12	0.04	522	5.17
0.4	17	0.04	515	4.68
0.45	15	0.04		5.59
0.5	12	0.04	518	4.76

3.2.2 Turbidity after PEI treatment

Comparing the homogenate and the heat-treated homogenate with- and without PEI treatment clear results in terms of turbidity were obtained and are shown in Figure 17:
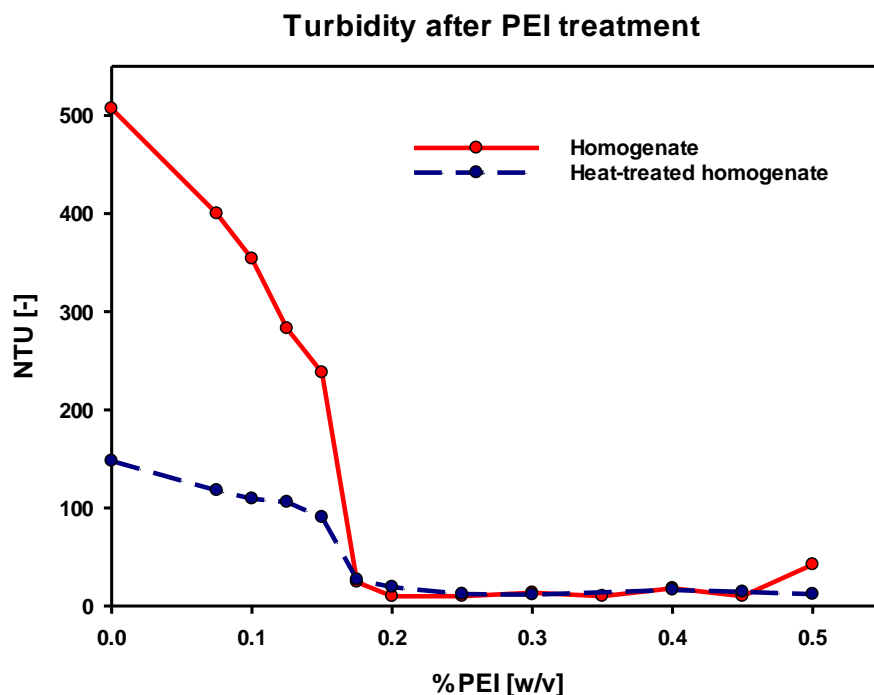
Figure 17: Turbidity after PEI treatment: Homogenate and Heat precipitate

Before PEI treatment, the turbidity of the clarified homogenate was approx. 500 NTU whereas the turbidity of the clarified heat- treated homogenate was approx. 150 NTU. The differences can be explained by the irreversible aggregation of the heat- unstable proteins due to the long- time heat exposure of the homogenate. With the addition of PEI the turbidity

decreased due to the polymer bridging i.e. the flocculation of the negatively charged cell debris and other negatively charged host cell components. Comparing the homogenate and the heat-treated homogenate after PEI treatment, the decrease of turbidity was more pronounced for the homogenate which decreased from 500 to 400 after the addition of 0.075% PEI. After 0.1% PEI addition the turbidity decreases to 354 NTU; after the addition of 0.125% PEI it decreases to 283 NTU and after addition of 0.15% it decreased to 238 NTU. The strongest decrease of turbidity occurred after the addition of 0.175% PEI. At this PEI concentration the turbidity dropped to 24 NTU and it seems to be that there is a PEI concentration, where most of the particles are flocculated by the polymer and almost no turbidity is left. An addition of 0.2% PEI led to a further decrease to 10 NTU and remained constant until 0.5% PEI where an increase of turbidity to 42 NTU was observed. Considering the heat- treated homogenate after PEI treatment, the decrease of the turbidity was much less from 150 NTU to 120 NTU after 0.075% PEI addition, to 110 NTU after 0.1% PEI, to 106 NTU after 0.125% PEI and to 91 after 0.15% PEI. In the same way, as the homogenate, the strongest decrease of turbidity was observed after the addition of 0.175% PEI where the turbidity decreased to 27 NTU and was almost equal to the turbidity of the homogenate. Further addition of PEI led to a decrease of the turbidity to 10 NTU after 0.2% PEI and remained almost constant.

3.2.1 DNA levels after PEI treatment

DNA levels of homogenate and heat-treated homogenate after the addition of PEI is shown in Figure 18:
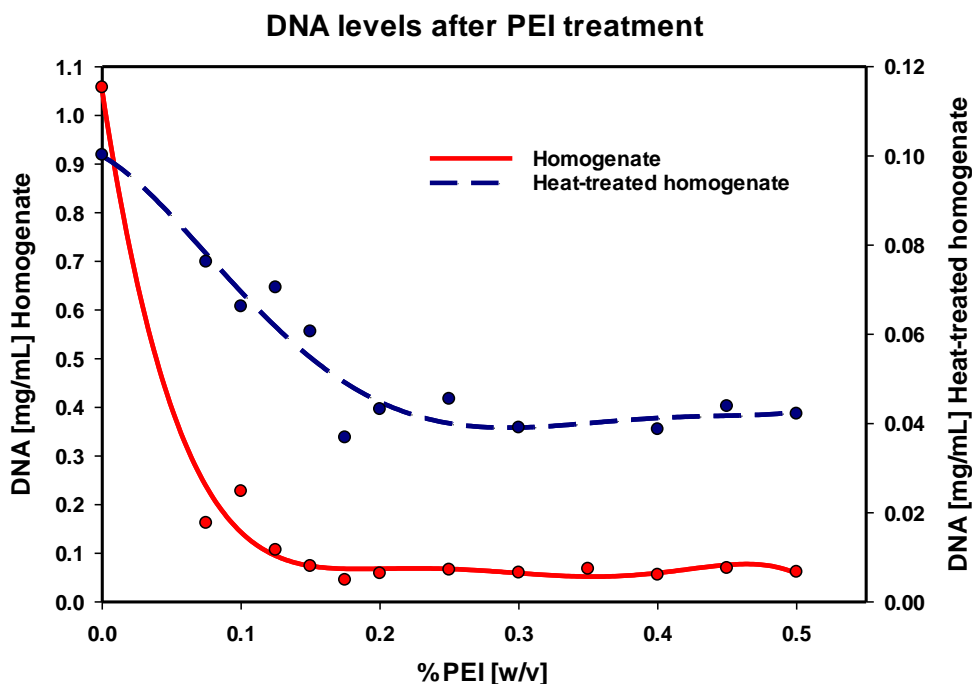
Figure 18: DNA after PEI treatment: homogenate and heat-treated homogenate

Before PEI treatment, the clarified homogenate had a DNA concentration of 1.1 mg/mL whereas the clarified heat-treated homogenate had a DNA concentration of 0.1 mg/mL. As already mentioned in section 1.2.3 the thermal stability i.e. the melting temperature of DNA depends on their size and rearrangement in solution and is typically between 50- and 100 °C. By the comparison of the homogenate and the heat-treated homogenate, the long- time heat exposure led already to a reduction of DNA of approx. 90% which means that most of the DNA was irreversible degraded i.e. aggregated at these conditions. After the addition of the lowest PEI concentration which was 0.075%, to the homogenate, a major reduction of the DNA level to a concentration of 0.15 mg/mL was observed indicating that the PEI is very selective to the DNA fragments. Further addition of PEI led also to further DNA reduction with the lowest level of 0.015 mg/mL measured after 0.175% PEI addition and constant low DNA concentrations after further PEI addition. Comparing the heat-treated homogenate after PEI treatment, the DNA reduction was much stronger simply due to the higher start concentration. The lowest DNA concentration was also measured after the addition of 0.175% PEI with 0.04 mg/mL and remained almost constant after further PEI addition.

3.2.2 Endotoxin levels after PEI treatment

Due to elaborate sample preparation for endotoxin measurement less samples were measured after PEI treatment but by the comparison of the homogenate and the heat-treated homogenate with- and without PEI treatment also clear results were obtained which are shown in Figure 19:
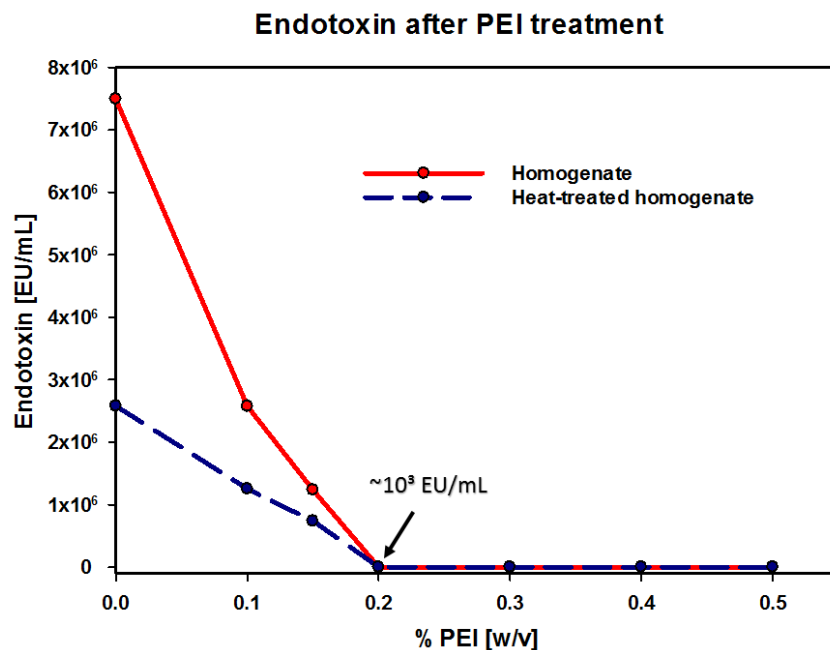
Figure 19: Endotoxin after PEI treatment: Homogenate and Heat-precipitate

51

Before PEI treatment the clarified Homogenate had an endotoxin concentration of 7.5 million EU/mL whereas the clarified Heat- precipitate had an endotoxin concentration of 2.6 million EU/mL. This result is a little bit surprising since endotoxins are very stable molecules and it actually not assumed that a heat- treatment with 50 °C is sufficient to reduce the endotoxin content to 1/3 compared to the starting solution. However, the precipitation of heat-labile proteins might induce co-precipitation of endotoxins. The addition of 0.1% PEI to the homogenate resulted in a reduction of endotoxin concentration to 2.5 million EU/mL. The endotoxin concentration was further reduced to 1.2 million EU/mL upon increasing PEI concentration at 0.15% PEI and to 600 EU/mL at 0.2% PEI. A further increase of PEI concentration didn`t led to further Endotoxin reduction. For the heat-treated homogenate, the PEI addition also led to an endotoxin reduction but the reduction was lower compared to the Homogenate. An addition of 0.1% PEI led to an endotoxin concentration of 1.25 million EU/mL. The endotoxin concentration was further reduced to 700,000 EU/mL at 0.15% PEI and to 1000 EU/mL after 0.2% PEI. A further increase of PEI concentration didn`t led to further endotoxin reduction.

3.2.3 Comparison of homogenate and heat-treated homogenate after PEI treatment

Comparing the results of the homogenate- and the heat-treated homogenate a similar trend was observed for turbidity, DNA- and endotoxin concentration. The starting concentrations for the homogenate was always higher and the addition of low PEI concentrations led to higher reduction compared to the heat-treated homogenate. At a PEI concentration of 0.175% there was almost no difference between the homogenate and the heat-treated homogenate in terms of DNA concentration and turbidity. This PEI concentration seems to be sufficient as most of the negatively charged bioparticles were precipitated and flocculated. The endotoxin concentration was not measured at this PEI concentration but it is suspected that this also valid for the endotoxins. In this case, the endotoxin concentration had reached the lowest level at 0.2% PEI addition and remained constant. As already mentioned, GFP is also negatively charged at a pH of 8 but seems to be not affected by the PEI since no protein loss was observed in any flocculation experiment.

3.2.4 PEI flocculation of homogenate and heat-treated homogenate – 250 mL scale

In order to be able to use the PEI treated homogenate- and heat-treated homogenate for the following purification steps i.e. adsorption isotherms, batch adsorption and breakthrough experiments on the CaptoQ resin, the scale up had to be studied. Furthermore, ultra-and diafiltration was performed to prepare samples at appropriate GFP concentration and buffer conditions. Based on the small scale experiments a 0.3% (w/v) PEI concentration was chosen due to the assumption that an effective reduction of DNA and endotoxin is definitely reached at this concentration. Figure 20 shows the results of the turbidity measurement after PEI treatment:
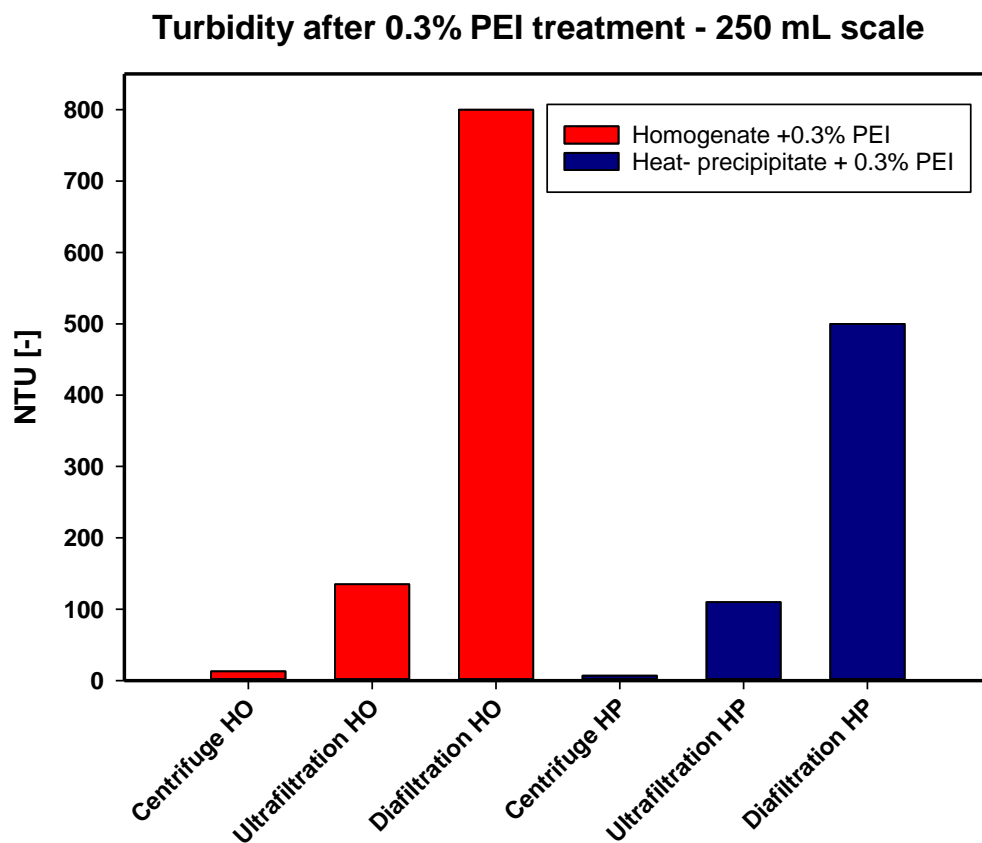
Figure 20: Turbidity after 0.3% PEI treatment – 250 mL scale

As can be seen in Figure 20, a high increase of turbidity after ultra- and diafiltration was observed. Additionally, complete membrane blocking after approx. 4 volume exchanges and loss of GFP was observed. The DNA concentration with approx. 0.02 mg/mL and the endotoxin concentration with less than 200 EU/mL shows, that a successful reduction had been reached. In terms of filtration process it is suspected that residiual surplus PEI is in the protein solution or weak reversible bound PEI is dissociated from the flocculated cell debris and causes the high increase of the turbidity. It is also suspected that dissociation is strongly

reinforced by the conductivity change during diafiltration where the 50 mM, Tris 50 mM NaCl buffer at pH 8 was exchanged by a 10 mM Tris buffer at pH 7.5. This assumption is supported by the comparison to the small scale experiments where the untreated clarified homogenate- and heat-treated homogenate had a much lower turbidity compared to the PEI treated samples. Based on these results it was decided to choose a PEI concentration on the lower limit, where an effective reduction was achieved according to the small scale experiments. Therefore a PEI concentration of 0.2% (w/v) was used for the following experiments. Figure 21 shows the turbidity results for homogenate and the heat-treated homogenate:
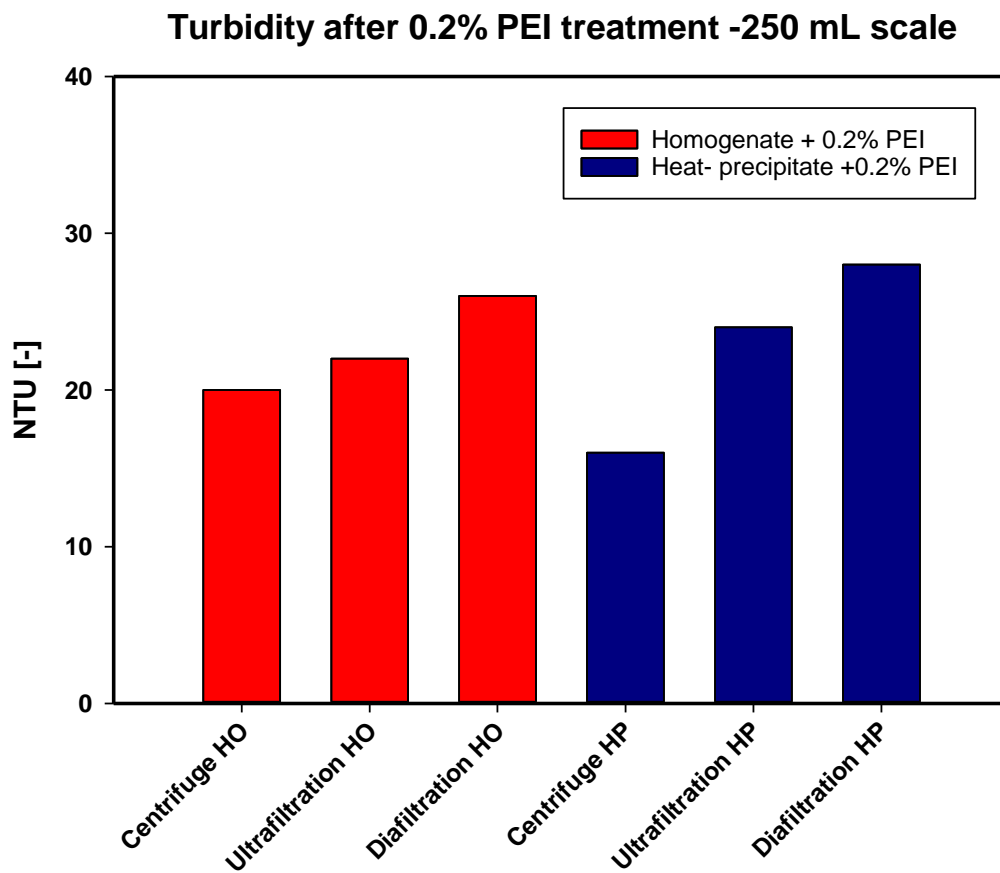
Figure 21: Turbidity after 0.3% PEI treatment – 250 mL scale

Comparing the results, the turbidity increased from ultra- to diafliltration but almost negligible. The permeate flow was measured with approx. 50 L/m^{2}h for both samples in the diafiltration process and no membrane blocking was observed. Additionally little loss of protein was observed but the desired protein concentration of approx. 10 mg/mL was reached. The DNA- and endotoxin concentration were in a similar range as measured for the 0.3% PEI treated samples.

3.3   Adsorption isotherms

Adsorption Isotherms i.e. the determination of equilibrium parameters provide important information necessary for interpretation of kinetic data. Therefore, the first experimental approach to investigate adsorption behaviour of GFP, DNA and endotoxin on the anionic exchange resin CaptoQ are adsorption isotherms. This was performed for a homogenate (HO), a heat-treated homogenate (HP), a homogenate, which was treated with 0.2% PEI HO+PEI) and a heat-treated homogenate which was treated with 0.3%PEI (HP+PEI). All samples were ultrafiltrated to obtain similar starting concentration of GFP and diaifiltrated to avoid electrostatic interactions between the ions of the homogenisation buffer as well as residual small molecular weight components of the fermentation broth and the charged ligands of the CaptoQ resin. The tables of result are showed in section 9. Table 15 summarises the starting concentration of GFP, DNA and endotoxin. To study also the adsorption behaviour of ultrafiltrates after PEI treatment, one experimental approach was performed with PEI treated samples. These samples were not from the same batch and the PEI concentration was also a little different. The heat-treated homogenate was treated with 0.22%PEI ultrafiltrated to 10 mg/mL GFP and afterwards diluted 1.2 with dH_2O to reduce the conductivity. The homogenate was treated with 0.2% PEI ultrafiltrated to 10 mg/mL GFP and afterwards diluted 1.2 with dH_2O to reduce the conductivity. The experimental setup had already been shown in 2.7.3.

Table 15: Starting concentrations for adsorption isotherms

	HO	HP	HO+PEI	HP+PEI	HO+PEI UF	HP+PEI
GFP [mg/mL]	9.63	10.65	9.82	9.72	4.95	4.8
DNA [mg/mL]	1.13	0.092	0.024	0.021		
Endotoxin [mg/mL]	0.25	0.142	$2*10^{-6}$	$3*10^{-6}$		

3.3.1 Adsorption isotherms – diafiltrated homogenate

Considering the adsorption behaviour at equilibrium of the GFP of the diafitrated homogenate which is shown in Figure 22, a Langmuir isotherm or type I adsorption isotherm was observed at low protein concentration. The maximum binding capacity of 90 mg/mL was reached at 0.33 mg/mL GFP and remained almost constant until 2.88 mg/mL. At higher concentration a strong decrease in the binding capacity of GFP was observed. At a measured GFP concentration of 7.4 mg/mL, the binding capacity dropped to 40 mgGFP/mL and a further decrease to 20 mgGFP/mL was observed at 8.5 mg/mL. At that point, where the binding capacity of GFP started to drop, the binding capacity of DNA and endotoxin increased indicating that these components have displaced the GFP out of the resin. To highlight this behaviour, the binding capacities of DNA and endotoxin are shown at the measured GFP concentration in the supernatant.
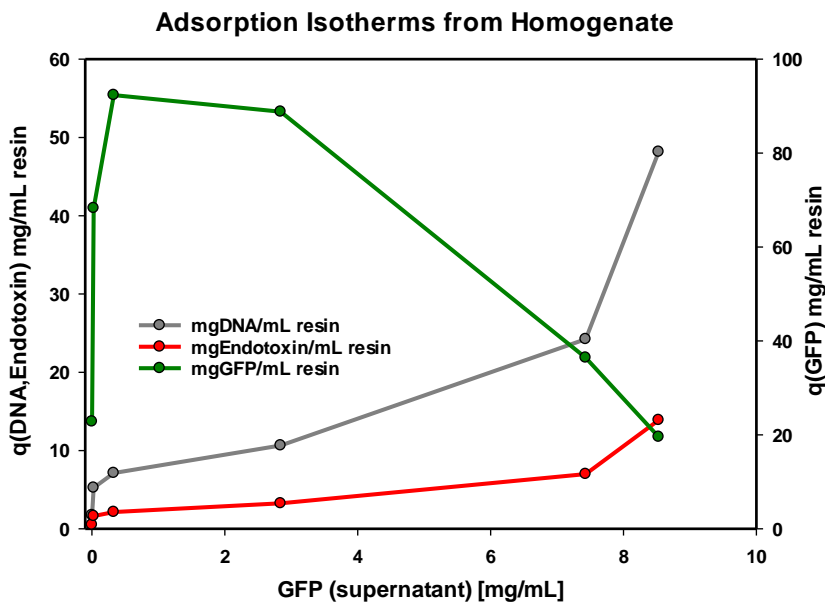
Figure 22: Adsorption Isotherm from Homogenate: GFP, DNA and Endotoxin

The real shape of the adsorption isotherms of endotoxin and DNA is shown in Figure 23
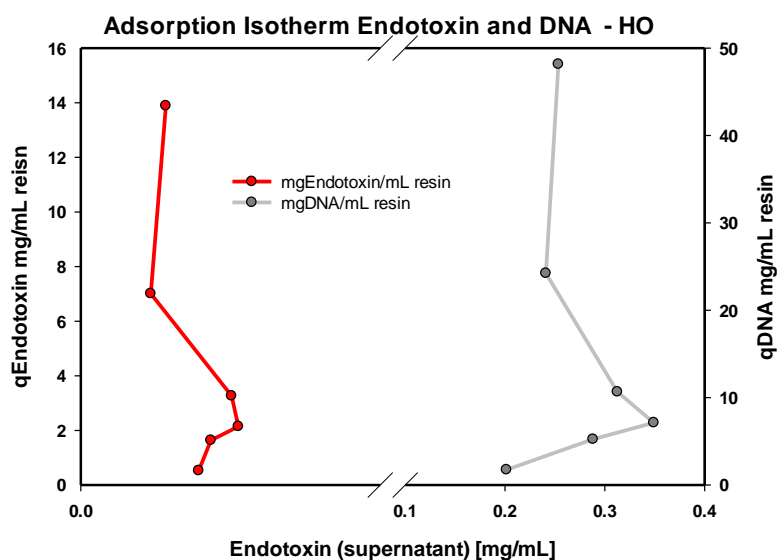
Figure 23: Adsorption isotherms: Endotoxin and DNA from HO

Considering the adsorption isotherms of DNA and endotoxin a similar shape was observed which appears to be a Langmuir adsorption behaviour but no saturation was reached. In another perspective, there is also the possibility, that the shape of the isotherms, especially that of the DNA is actually a type 3 isotherm. This behaviour cannot be verified in this experimental setup, since the DNA concentrations are on the lower limit of detection and a measurement of a DNA of 0 mg/mL is not possible with the used DNA assay. What can be observed is, that at a certain DNA and Endotoxin concentration a sudden, strong increase of binding capacity was measured with the highest binding capacity of 14 mg/mL resin for endotoxin and 48 mg/mL resin for DNA.

3.3.2 Adsorption isotherms – heat-treated homogenate

For the heat-treated and diafiltrated homogenate, a typical Langmuir adsorption behaviour was obtained at low protein concentrations. A steep linear increase of binding capacity at low protein concentration which reached maximum binding capacity of 200 mg/mL at 0.8 mg/mL GFP. The binding capacity remained almost constant until 2.4 mg/mL GFP in the supernatant but then decreased continuously at higher protein concentration. The lowest binding capacity of 37 mg/mL resin was obtained at a GFP concentration of 10.26 mg/mL. Along with decreasing binding capacity of GFP, the binding capacity of DNA and endotoxin increased. For demonstration purposes, the binding capacity of DNA and endotoxin is plotted against the GFP concentration in the supernatant and is shown in Figure 24. Apparently, there is a linear increase until 9.5 mg/mL GFP in the supernatant where the binding capacity of the endotoxin was 7.6 mg/mL resin and was almost doubled to 13.8 mg/mL resin at 10.26 mg/mL GFP.
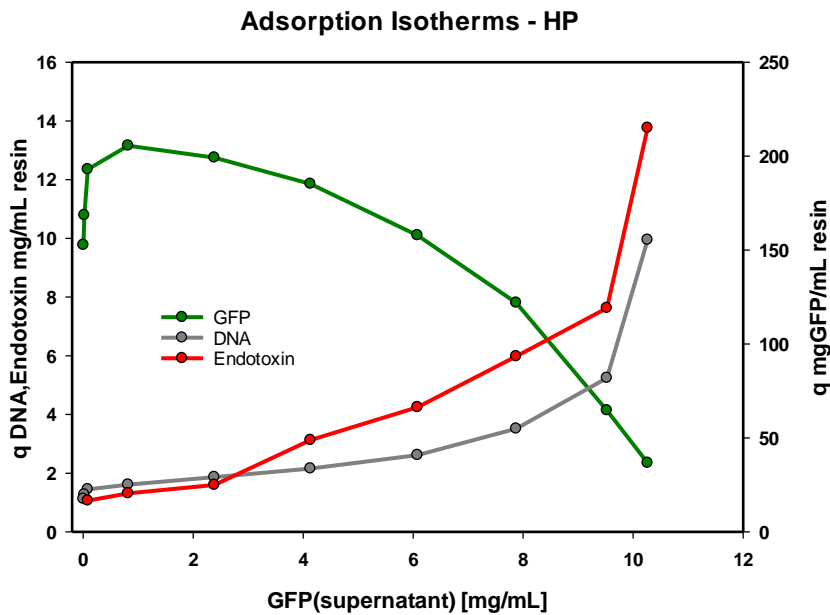
Figure 24: Adsorption Isotherms from Heat-precipitate: GFP, DNA and Endotoxin

At this point the binding capacity of the GFP was the lowest. For DNA, there was also a linear increase in binding capacity with increasing GFP concentration but the slope was smaller compared to endotoxin binding capacity. Same as for the endotoxin, the binding capacity of DNA was almost doubled from 5.2 to 10 mg/mL resin at the highest GFP concentration. The true shape of the isotherms of DNA and Endotoxin is shown in Figure 25
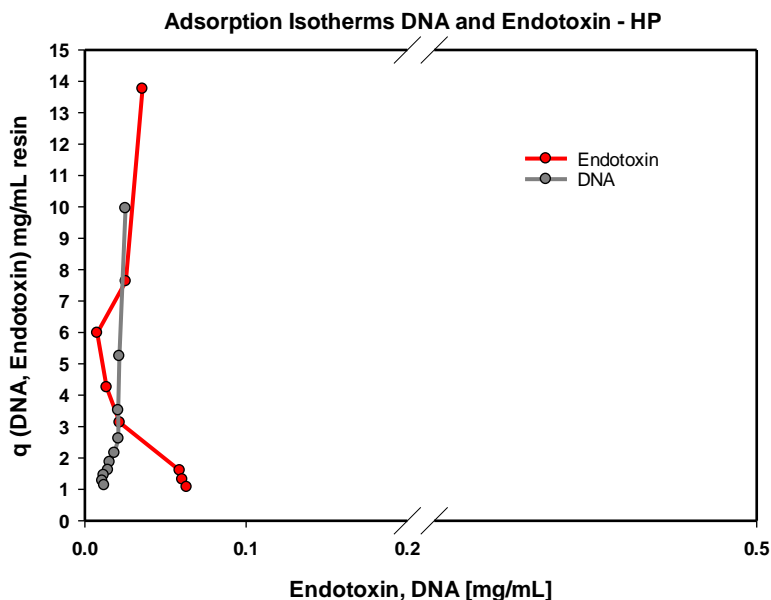
Figure 25: Adsorption Isotherms: DNA and Endotoxin from Heat-precipitate

Considering the adsorption behaviour DNA and Endotoxin, the shape of the isotherms are apparently Langmuir type isotherm which do not reach saturation but there is also the presumption especially in the case of the DNA that it is actually a type 3 adsorption behaviour. This presumption is magnified when the bound DNA was eluted with 1 M NaCl and the binding

capacity calculated with the mass balance of bound and unbound DNA. The result is shown in Figure 26.

Eluted Adsporption Isotherm - DNA
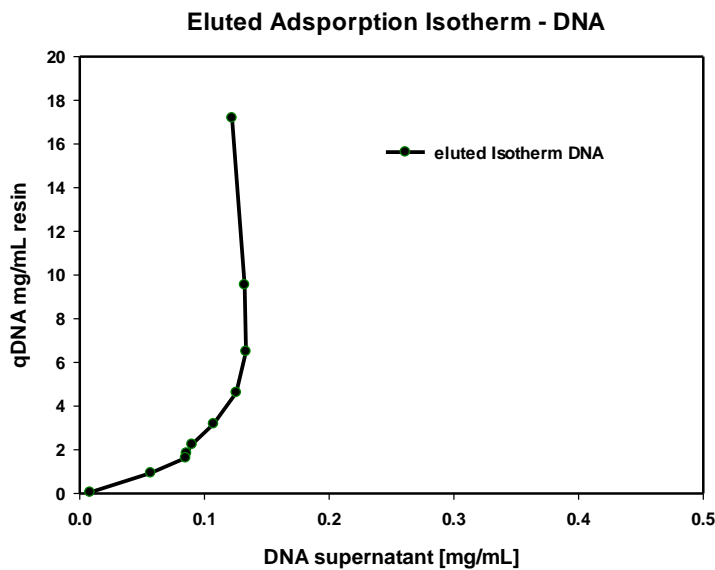
Figure 26: Adsorption Isotherm: DNA eluted

3.3.3 Adsorption isotherms – diafiltrated homogenate and- heat-treated homogenate after PEI treatment

For both samples, homogenate (HO+PEI) and heat-treated homogenate (HP+PEI) after PEI treatment, highly favourable isotherms were obtained. The isotherms after least sum of square fitting including the measurement points are shown in Figure 27. Ka value was obtained with 4930 mL/mg for HO+PEI and 2130 mL/mg for HP+PEI respectively. q_{max} was obtained with 256 mg/mL for HO+PEI and 232 mg/mL for HP+PEI.

Adsorption Isotherms PEI - GFP
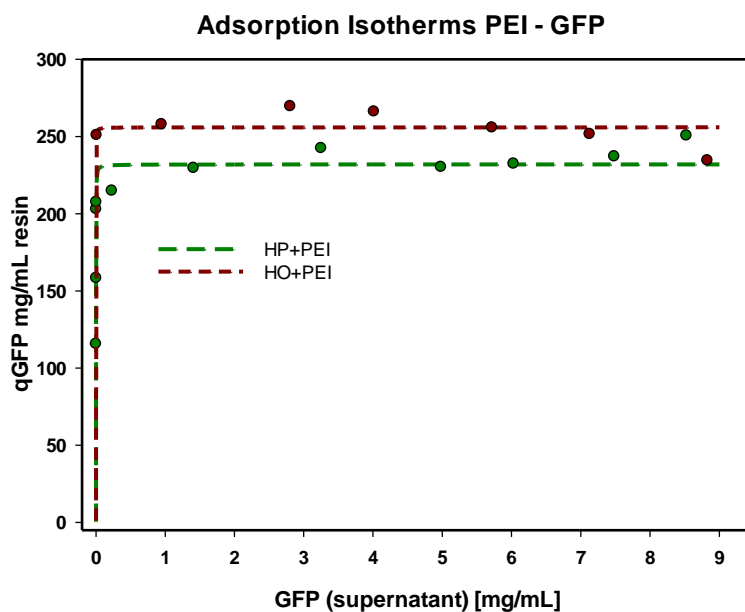
Figure 27: Adsorption Isotherms: HO+PEI, HP+PEI

Due to the low starting concentration of 0.024 mg/mL for the heat-treated homogenate and 0.021 mg/mL for the homogenate very low binding capacities with the highest of approx. 0.6 mg/mL resin for both samples were obtained. With respect to the shape of the isotherms which is shown in Figure 28, there is the presumption that the DNA shows a type 3 adsorption behaviour but especially at the low DNA concentrations, a limit of quantification was reached which makes it difficult to verify this hypotheses.
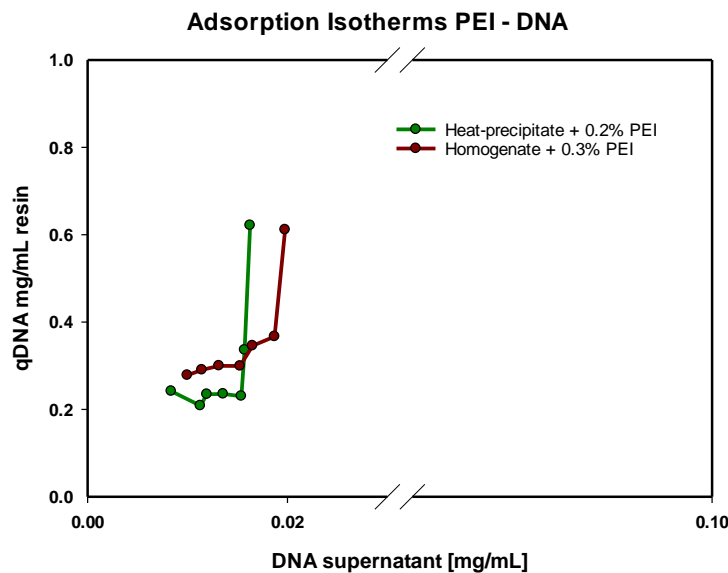
Figure 28: Adsorption Isotherms DNA: Homogenate + 0.3% PEI and Heat- precipitate + 0.2% PEI

3.3.4 Adsorption isotherms – ultrafiltrated homogenate and heat-treated homogenate after PEI treatment

Evaluation of the adsorption isotherms after ultrafiltration with subsequent dilution instead of diafiltration were studied as process option. The result are shown in Figure 29. For both samples, homogenate (HO+PEI UF) and heat-treated homogenate (HP+PEI UF) after PEI treatment, lower K_a and q_{max} values were obtained, compared to the diafiltrated samples. The HO+PEI UF led to a q_{max} of 114 mg/mL and a K_a of 50 mL/mg. HP+PEI UF led to a q_{max} of 153 mg/mL and a K_a of 22 mL/mg. Nevertheless, also the use of the homogenate without ultrafiltration (since the ultrafiltrate is diluted) is a promising alternative because a whole unit operation could be skipped. This would lead to other optimisation experiments for instance the use of a lower salt concentration in the homogenisation buffer.
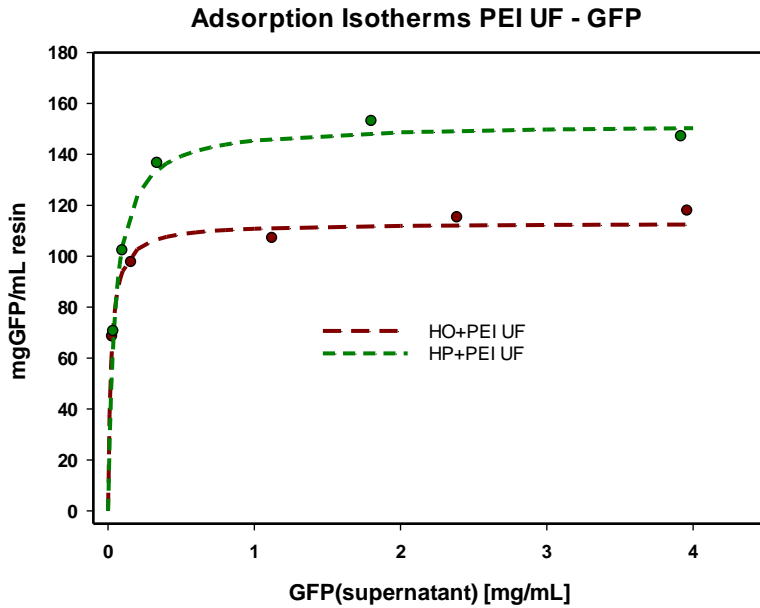
Figure 29: Adsorption Isotherms of diluted Ultrafiltrates: HP+PEI and HO+PEI

3.3.5 Comparison of the Adsorption isotherms

When comparing the adsorption isotherms of the homogenate and the heat-treated homogenate a high increase of binding capacity was observed after heat-treatment. This can be explained by the higher purity after precipitation of the heat labile components including the DNA which was also depleted to approx. 10% of the starting concentration. This can be seen clearly in Figure 30. But both samples showed a decrease in binding capacity with increasing protein concentrations and almost no binding capacity left at the highest protein concentrations. Therefore it is clear, that a single component adsorption is not the case and a Langmuir model for single component system is not sufficient to describe this adsorption behaviour. This is highlighted in Figure 31, where the experimental results were fitted with the Langmuir Model for single component system
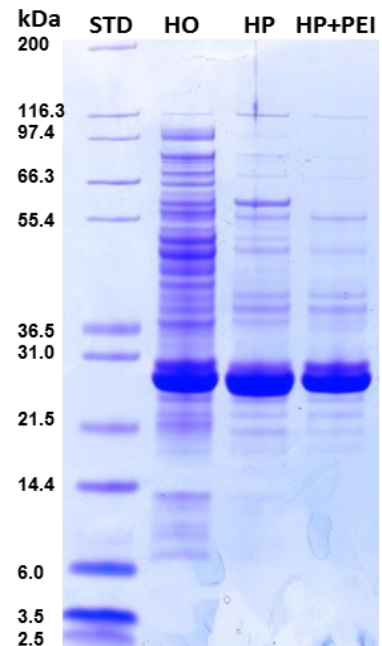
Figure 30: SDS PAGE: Homogenate (HO), Heat-precipitate (HP) and Heat-precipitate and PEI treatment (HP+PEI)

using least sum of square calculation. In both experimental setups, the binding capacities of DNA and the endotoxin were increasing, at the point where GFP was decreasing indicating that these two components are the responsible components displacing the GFP. This hypotheses is affirmed by the use of PEI after heat-treatment. Not only that the PEI treatment led to an additional increase of binding capacity but also the binding capacity remained almost constant over the whole GFP concentration range. Therefore the Langmuir Model is useful to describe it`s adsorption. Also by comparing the SDS PAGE of the HP and HP+PEI, no great

difference were obtained except one band at approx. 60 kDa which disappeared after the PEI treatment. The big difference after the PEI treatment compared to the homogenate and the Heat-treated homogenate is the strong depletion of DNA and endotoxin. The binding capacity of endotoxin was negligible after PEI treatment since the starting concentration was only 26 EU/mL which corresponds to 2.6 ng/mL. The binding capacity of DNA was only 0.6 mg/mL resin and should not have much influence on the adsorption especially when comparing this with the HO where the highest capacity was 48 mg/mL and the HP where the highest capacity was 10 mg/mL. One big question is the actual shape of the isotherms of DNA and endotoxin. For HO, the shapes of DNA and endotoxin could be Langmuir type, where saturation is not reached, but there is also the presumption of a type 3 adsorption isotherm. The problem to solve this question is the scaling due to low concentration after adsorption especially for DNA and connected with that the limit of quantification. In terms of Endotoxin high dilution of up to 1 to 10^6 are necessary, which can easily lead to dilution errors and therefore fluctuations in the binding capacities. But there are some observations which support the presumption of a type 3 adsorption behaviour. The first observation is that there is always a high increase of binding capacities in the last measurement points with a doubling of binding capacity from the second last to the last measurement point. The second observation is that of the eluted Isotherm of the HP. In this case, it seems that there are no outlier in this series of measurements leading to the shape of a type 3 adsorption isotherm.
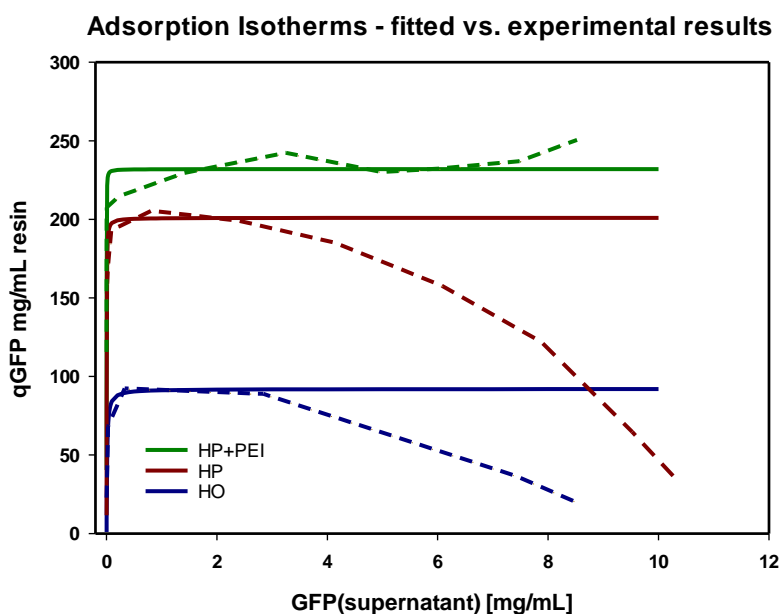

Figure 31: Adsorption Isotherms: experimental results and least sum of square fitting

3.4   Batch adsorption

To investigate the kinetics of the displacement effect, a batch adsorption experiment was performed for a diaflitrated homogenate (HO), a diafiltrated heat-treated homogenate (HP) and a diafiltrated heat-treated homogenate with 0.2%PEI (HP+PEI). The results of the measurements are summarised in Table 29 for HO and HP and in Table 30 for HP+PEI in section 9. Due to long sample preparation, the diafiltrated homogenate with PEI treatment was not investigated. The setup for the batch adsorption had already been shown in Table 7.

3.4.1   Batch adsorption – diafiltrated homogenate

The starting concentration of GFP, DNA and endotoxin are shown in Table 16. The batch adsorption for 60 min and the full time range in shown in Figure 32:

Table 16: starting concentration for batch adsorption HO: GFP, DNA, Endotoxin

Diafiltrated Homogenate - HO	
GFP [mg/mL]	9.16
DNA [mg/mL]	0.95
Endotoxin [mg/mL]	0.29
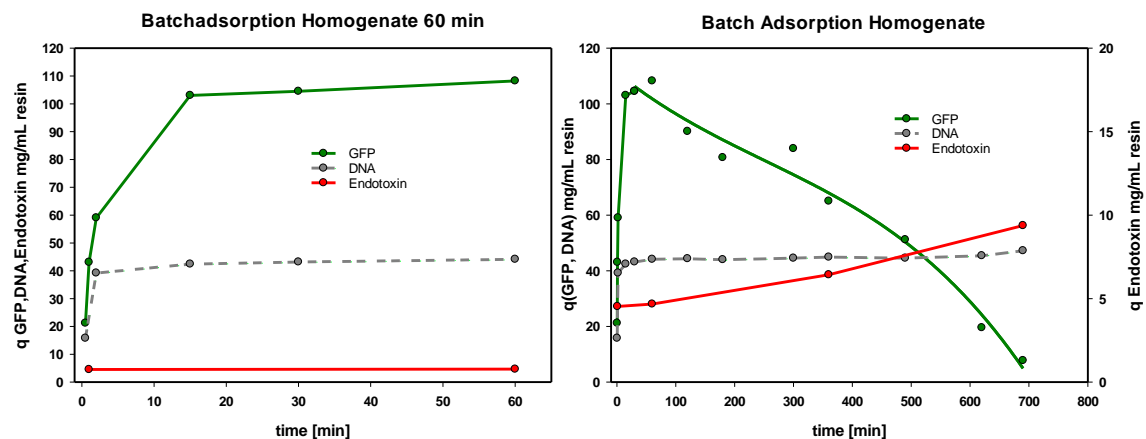
Figure 32: Batch adsorption HO: (left) 60 min; (right) full time range

Adsorption of GFP in the homogenate showed a maximum capacity of 103 mg/mL after 15 min. The capacity remained apparently constant until 60 min and thereafter decreased continuously to a minimum of 8 mg/mL after 690 min. Initial DNA adsorption occurred rapidly and reached 16 mg/mL after 30 seconds. After 2 min a capacity of 39 mg/mL was obtained. Afterwards a slow increase to 45 mg/mL was observed. Adsorption kinetics of endotoxins were qualitatively similar with rapid initial adsorption. But in contrast to DNA adsorption, endotoxin binding capacity was doubled from 5 mg/mL after 1 min to 10 mg/L after 690 min. This corresponds to 61% of bound endotoxins

3.4.2 Batch adsorption – heat-treated homogenate

The starting concentration of GFP, DNA and endotoxin are shown in Table 17. The batch adsorption for 60 min and the full time range are shown in Figure 33:

Table 17: starting concentration for batch adsorption HP: GFP, DNA, Endotoxin

Diafiltrated heat-treated homogenate -HP	
GFP [mg/mL]	10.08
DNA [mg/mL]	0.25
Endotoxin [mg/mL]	0.28
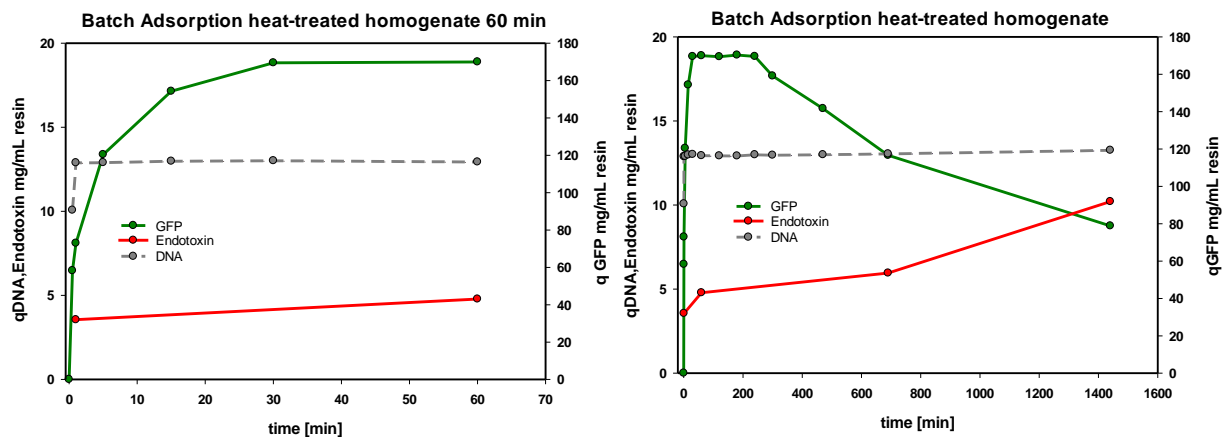
Figure 33: Batch adsorption – HP: (left) 60 min; (right) full time range

Adsorption kinetics of GFP, DNA and endotoxins from HP followed almost exactly the same trends as the HO. However, binding capacities for GFP were higher and displacement was somewhat less pronounced and slower. Also in this case fast initial adsorption of DNA and endotoxin was observed. However, binding capacities of DNA were 2-3 lower compared to the HO due to lower starting concentrations, whereas endotoxin adsorption was almost exactly the same.

3.4.3 Batch adsorption – heat and PEI treated homogenate

The batch adsorption of GFP from HP+PEI is shown in Figure 34. The starting GFP concentration was determined with 9.5 mg/mL. The binding capacity after 0.5 min was determined with 107 mg/mL resin and increased continuously to 245 mg/mL after 30 min. After 60 min, the adsorption gradually approached saturation where the binding capacity was 284 mg/mL resin. After 120 min the binding capacity was slightly increased to 293 mg/mL resin and remained constant from 240 min to 1440 min, where the binding capacity was 300 mg/mL resin. This apparently slow protein uptake which was obtained for the first 60 min does not fit to the highly favourable adsorption isotherms but the focus was set if displacement occurs or not. Therefore it is not further discussed but will be part of another experimental investigation.
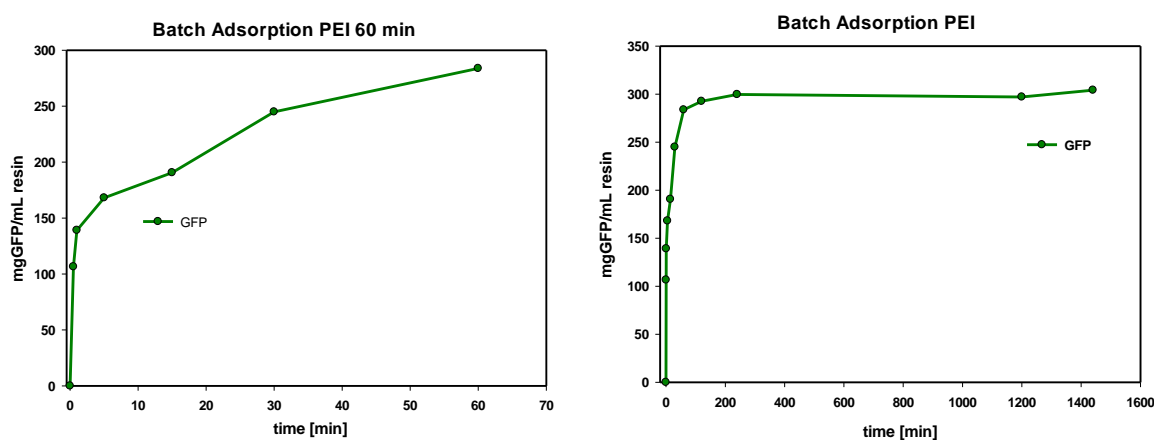
Figure 34: Batch adsorption HP+0.2%PEI (left) 60 min; (right) full time range

3.4.4 Comparison of Batch adsorption experiments

As expected, no displacement of GFP was observed at the PEI treated sample whereas displacement of HO and HP was very slow. The surprising result was the adsorption behaviour of DNA. As already mentioned, the free diffusivity of DNA is actually quite slow but this is only valid for larger DNA molecules. In this batch adsorption experiment it was shown, that the diffusion of DNA into the pores is really fast, as saturation was reached already after approx. 2 minutes. A possible explanation to this behaviour is the fragmentation of DNA after homogenisation. And it seems that the DNA fragments which diffuse into the pores are small. Another question which cannot be answered in this experiment is how far DNA diffuse into the pores. This question could be solved with the use of a confocal microscope analysis by staining the DNA fragments with the Hoechst dye and the measurement of fluorescent of the adsorbed DNA fragments in the resin particles. That was however not part of this work. But the biggest question is whether the DNA is a displacer of GFP. Considering only the results of the adsorption isotherms, the answer would be yes since there is a strong increase of DNA

binding capacity when the binding capacity of GFP drops. But considering the batch adsorption it looks like that there is a cooperative binding of GFP and DNA since both diffuse into the pores very fast. They have reached saturation and no increase of the DNA binding capacity was observed, when the GFP was displaced out of the resin. A possible answer could be the phase ratio or the accessible resin volume per sample volume. The highest increase of DNA binding capacity can be observed at the highest phase ratios. The highest phase ratios for the HP are 1:75 and 1:150 whereas the phase ratio of the batch adsorption is 1:40. This could also explain why the GFP is not fully displaced out of the resin and the binding capacity of 79 mg/mL resin remains after 24 hours. In this case, the DNA would be rather a competitive component, which reduces the binding capacity of GFP than a displacer of the GFP. Considering the adsorption behaviour of endotoxin the situation looks different. As already mentioned in 1.1.2, endotoxins have different arrangements in solution including monomers, dimers, micelles and vehicles but the actual arrangement in solution is hard to predict. Taking this information into consideration with the results of the batch adsorption experiment, it is suspected that free endotoxin monomers of approx. 10 kDa first diffuse into the pores. This is suspected because 25% of the endotoxins from the HO and 31% from the HP are bound after 0.5 minutes. Afterwards the adsorption increased much slower or remained constant for the first 60 min. A possible reason which is also stated by Hiryama et. al [54] is the steric exclusion of endotoxin aggregates i.e. the size of the micelles and vehicles which can only adsorb on the outer surface of the ion exchange particles. As already mentioned in 1.1.2 an equilibrium shift can lead to a release of endotoxin monomers from the aggregates. By combination of these two information it is hypothesised that the endotoxin aggregates are bound to the outer surface of the particles and release monomers into the pores, thereby displacing the GFP from the ligands due to higher electrostatic interactions. According to the batch adsorption experiment this mechanism would be a very slow process, since the increase of binding capacity from 4.7 mg/mL to 9.4 mg/mL took 10 hours for HO and 24 hours for HP to increase from 4.8 mg/mL to 10.2 mg/mL resin. The other question is, how many ligands are occupied by the endotoxin monomers after displacement and is this sufficient to displace all of the GFP as it is the case with the homogenate. This question cannot be answered and would need further investigations.

3.5 Anion Exchange Chromatography – Result overview of Breakthrough-curves

To investigate the adsorption behaviour of DNA and endotoxin in column operation mode, especially the influence of the flow rate, breakthrough experiment were performed. At 1.5 minutes and 9 minutes residence samples from HO, HP and HP+PEI were used. The samples were from the same starting solution as used in the batch adsorption experiment. The results of the single measurements are summarised in Table 31 and Table 32. The chromatograms are shown in Figure 35.
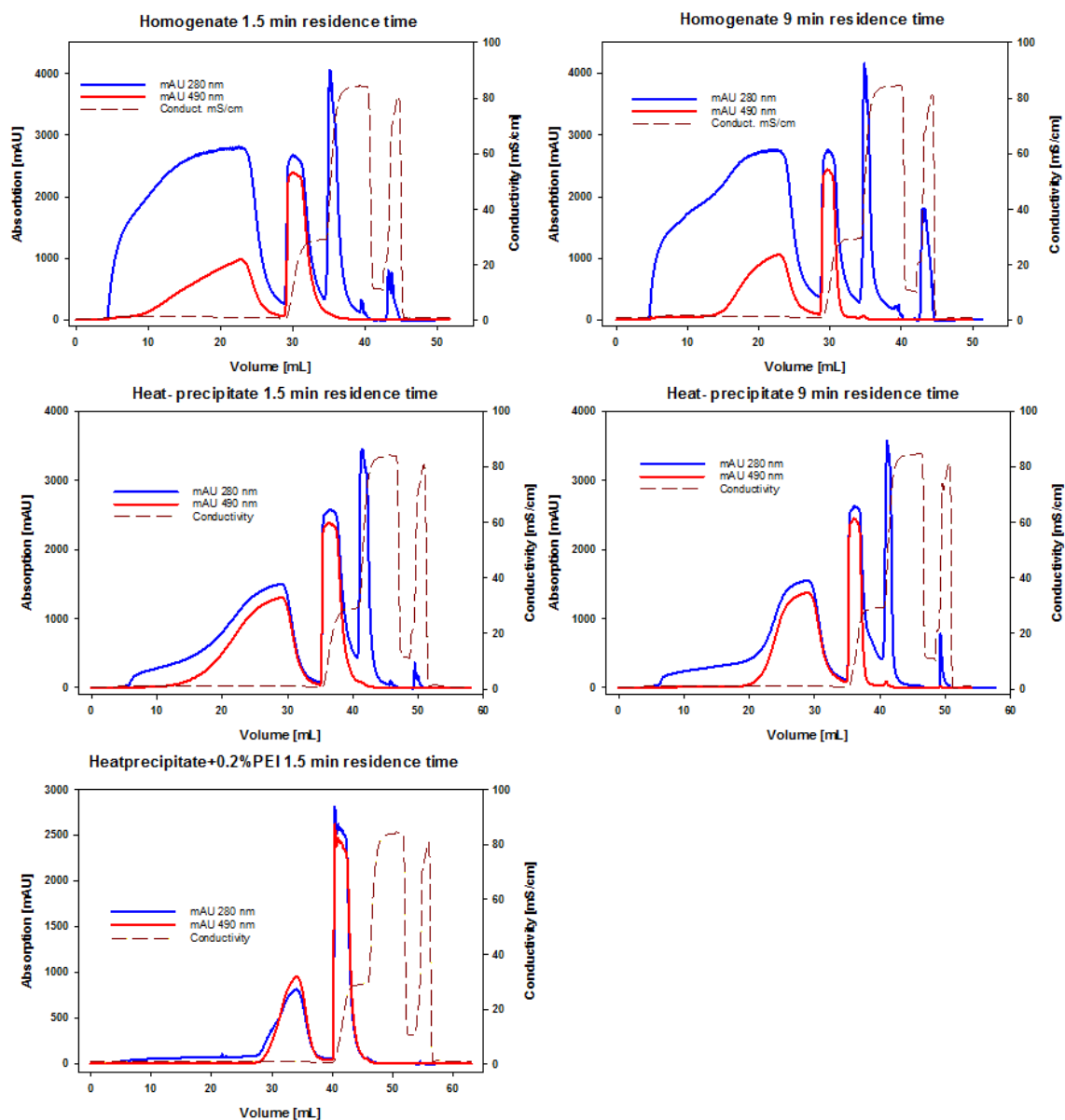
Figure 35: Chromatograms of breakthrough experiments: Homogenate, Heat-precipitate and Heat-precipitate+0.2%PEI at 1.5 min residence time left and 9 min residence time right

The setup had already been shown Table 8. GFP in break-through was calculated with UV490 nm in the bypass absorption compared to the UV490 nm absorption after the column. In addition, the breakthrough curve of GFP was fitted with the constant pattern solution for film and pore diffusion to obtain DBC at 10% breakthrough, effective pore diffusion- and film mass transfer coefficient.

3.5.1 Break-through curves - homogenate

The starting concentrations for GFP, DNA and endotoxin are shown Table 18. The results of the adsorption of endotoxin and DNA during GFP breakthrough are shown in Figure 36

Table 18: Starting concentrations for break-through experiments HO – GFP, DNA and endotoxin

Diafiltrated Homogenate - HO	
GFP [mg/mL]	9.16
DNA [mg/mL]	0.95
Endotoxin [mg/mL]	0.29
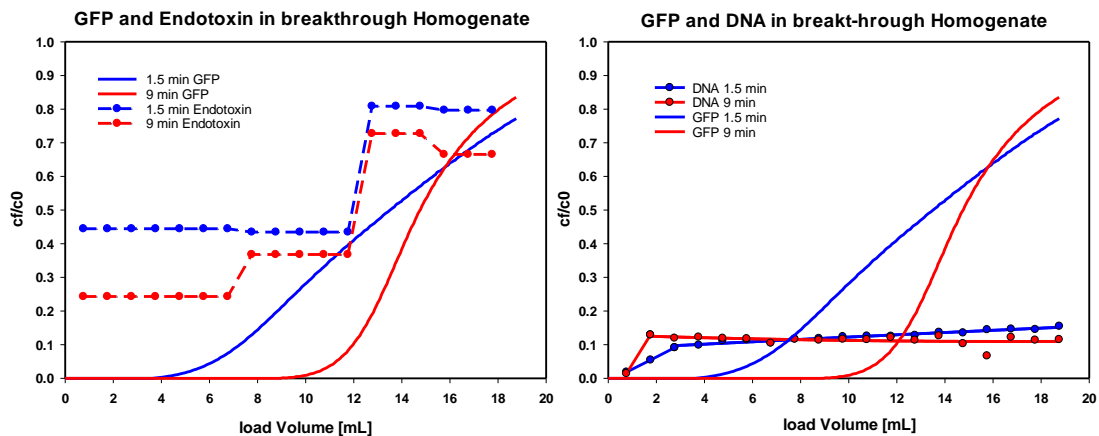
Figure 36: Endotoxin and DNA in GFP break-through- HO

Major differences between the two residence times for endotoxin adsorption were observed at the beginning of sample loading where the lower residence time showed a much higher breakthrough. After that, differences were less big but the lower residence time showed always a little higher breakthrough. In terms of DNA, almost no differences were observed between the two residence times. In both cases only about 10% of the total loaded DNA were found in the break-through

The mass balance of the break-through experiments including the recovery, which also takes elution steps into account, is summarized in Table 19.

Table 19: Mass balance of DNA and Endotoxin - HO

residence tme	Column load	load V [mL]	start c [mg/mL]	total load [mg]	in breakthrough [mg]	0.3 M NaCl [mg]	1 M NaCl [mg]	recovery [%]
1.5 min	DNA	17.85	0.95	17.0	2.09	0.39	0.18	16
	Endotoxin	17.85	0.29	5.2	2.95	0.06	0.06	59
9 min	DNA	17.85	0.95	17.0	1.97	0.27	0.09	14
	Endotoxin	17.85	0.29	5.2	2.25	0.06	0.147	51

In total, only about 15% of the DNA that was loaded could be recovered. This can be explained by strong binding of DNA onto the resin which probably could only be eluted after regeneration with sodium hydroxide.12% were found in the break-through but almost none of the total bound DNA was found in the elution steps. In terms of endotoxin, most was found in the break-through with 57% of the total bound endotoxin at 1.5 min and 43% at 9 min. This indicates a higher flow rate dependency of endotoxin adsorption. Similar to DNA elution, only very low amounts of endotoxins with respect to the total loaded amounts were found in the eluates. This also indicates that there is a strong irreversible binding of endotoxin.

3.5.2 Break-through curves – heat-treated homogenate

The starting concentrations for GFP, DNA and endotoxin are shown Table 20. The results of the adsorption of endotoxin and DNA during GFP breakthrough is shown in Figure 37.

Table 20: Starting concentrations for break-through experiments HP – GFP, DNA and endotoxin

Diafiltrated heat-treated homogenate -HP	
GFP [mg/mL]	10.08
DNA [mg/mL]	0.25
Endotoxin [mg/mL]	0.28
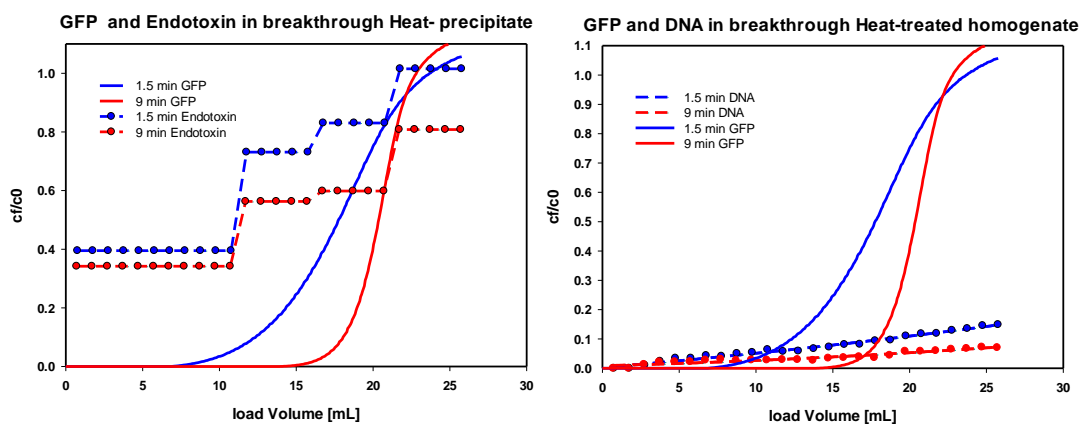
Figure 37: Endotoxin and DNA in GFP break-through- HP

For endotoxins, major differences were obtained after higher amount of sample had been loaded. At 1.5 min residence time, the breakthrough was always higher and a complete break-through was observed whereas at 9 min 80% break-through was observed. DNA in general showed little break-through for both residence times with the highest break-through of 15% at 1.5 min and 7% at 9 min.

The mass balance of the break-through experiments including the recovery, which also takes elution steps into account, is summarized in Table 21

Table 21: Mass balance of DNA and Endotoxin – Heat-treated homogenate

residence tme	Column load	load V [mL]	start c [mg/mL]	total load [mg]	in breakthrough [mg]	0.3 M NaCl [mg]	1 M NaCl [mg]	recovery [%]
1.5 min	DNA	25.76	0.25	6.5	0.48	0.13	1.93	39
	Endotoxin	25.76	0.28	7.3	4.76	0.06	0.06	67
9 min	DNA	25.76	0.25	6.5	0.24	0.08	1.10	22
	Endotoxin	25.76	0.28	7.3	3.75	0.04	0.147	54

In total 39% of the total bound DNA at 1.5 min residence time and- 22% at 9 min could be recovered. At 1.5 min 7% was found in the breakthrough, 2% was found in the 0.3 M elution step and 30% at the 1 M elution step. At 9 min 3.8% was found in the breakthrough 1.2% was found at 0.3 M elution step and 17% at 1 M elution. It is suspected that at both residence times, most of the DNA is strongly bound and elution is only possible after regeneration with sodium hydroxide. In terms of endotoxin, most of the recovery occurred in the breakthrough. At 1.5 min, 65% of the total bound endotoxin was recovered in the breakthrough, where also a total breakthrough of endotoxin was observed at the end of the loading step. At 9 min, 51% of the total bound endotoxin was found in the breakthrough, which was less compared to the 1.5 min but in this case a complete breakthrough was not observed. This also indicate a higher flow rate residence time dependency of endotoxin adsorption. Only small amounts were detected in the eluates.

3.5.3 Fitting of break-through curves - constant pattern solution for film and pore diffusion

By comparing HO and HP at the two different residence times, similar results were obtained. For DNA, the observed breakthrough is very low with approx. 10%. This results actually fits quite well to the results of the batch adsorption experiment, where complete binding was observed already after 1 min. The difference between the two residence times was marginal but a more distinct trend was observed for the HP, where breakthrough at 9 min was always approx. the half of the 1.5 min residence time. In all 4 chromatography runs, the recovery of the total loaded DNA was low and could be explained by strong binding between ligands and DNA which leads to elution mainly after regeneration with sodium hydroxide. This assumption was strengthened by the 1 M elution step of the HP, where a high DNA content was determined. Considering the endotoxin during GFP break-through also differences between the two different residence times were observed where a higher break-through was determined at 1.5 min for the HO and HP. However, these differences look different. In the HO, the main differences occurred at the beginning of loading, whereas the main differences of the HP were determined after a higher amount of sample loading. At 1.5 min also a complete breakthrough was observed. These results also fit to the batch adsorption experiments, where it was determined that diffusion of endotoxin into the resin is much slower compared to DNA but a part of the endotoxin is immediately adsorbed. This was tried to explain by endotoxin monomers, which can diffuse fast into the resin pores.

To investigate the influence of DNA and endotoxin on diffusional parameter of GFP, the film mass transfer coefficient k_f and the effective pore diffusion coefficient D_e were evaluated using the constant pattern solution for film and pore diffusion. In this case also the fit of the HP+PEI is shown. The results of the constant pattern solution for 1.5 min and for 9 min is shown in Figure 38. Unfortunately, the binding capacity for curve fitting of HP+PEI was underestimated for 9 min residence time and therefore missing in this evaluation due to not sufficient break-through. The results of the constant pattern solution including the experimental break-through curves are shown in Figure 43 in section 9.
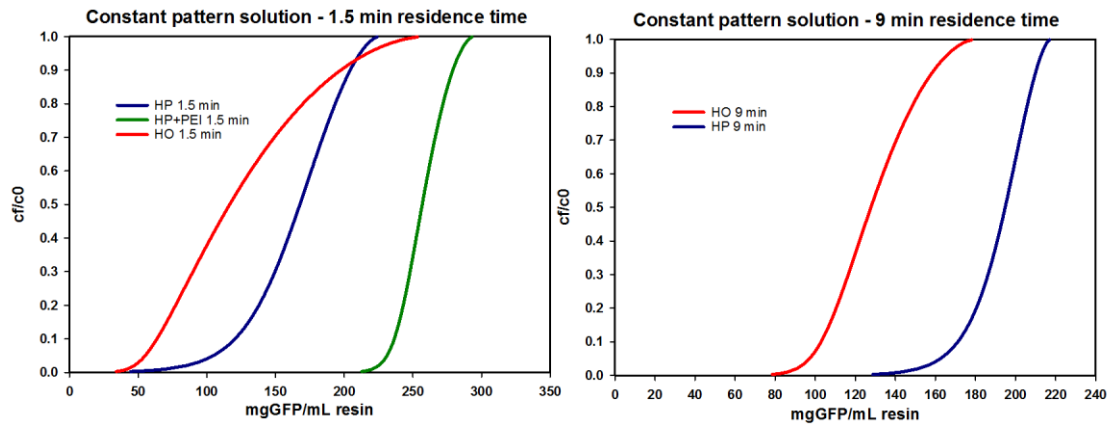
Figure 38: Constant pattern solution: left: 1.5 min residence time HO, HP, HP+PEI; right: 9 min residence time HO, HP

It had already been shown in the adsorption isotherm- and batch adsorption experiments that the HP+PEI had a much higher binding capacity than HP and HO. In column operation DBC at 10% break-through was used to confirm this results which are summarized in Table 22.

Table 22: Results of DBC at 10% break-through

	DBC10% [mg/mL resin]		
residence time [min]	HO	HP	HP+PEI
1.5	64	120	236
9	103	171	

Another important aspect in this investigation is the film mass transfer. By the use of the constant pattern solution it was found out that especially the adjusted k_f values showed high deviations from that which were calculated with Equation 10 for HO and HP. For HP+PEI the value predicted by the correlations was in agreement with the experimental data. This is highlighted in Figure 39. The results are summarised in Table 23

Table 23: Adjusted kf values from constant pattern solution for film and pore diffusion

	k_f [cm/h]		
residence time [min]	HO	HP	HP+PEI
1.5	$5 *10^{-4}$	$1.9 *10^{-4}$	10^{-3}
9	$9*10^{-5}$	$6.5 *10^{-5}$	
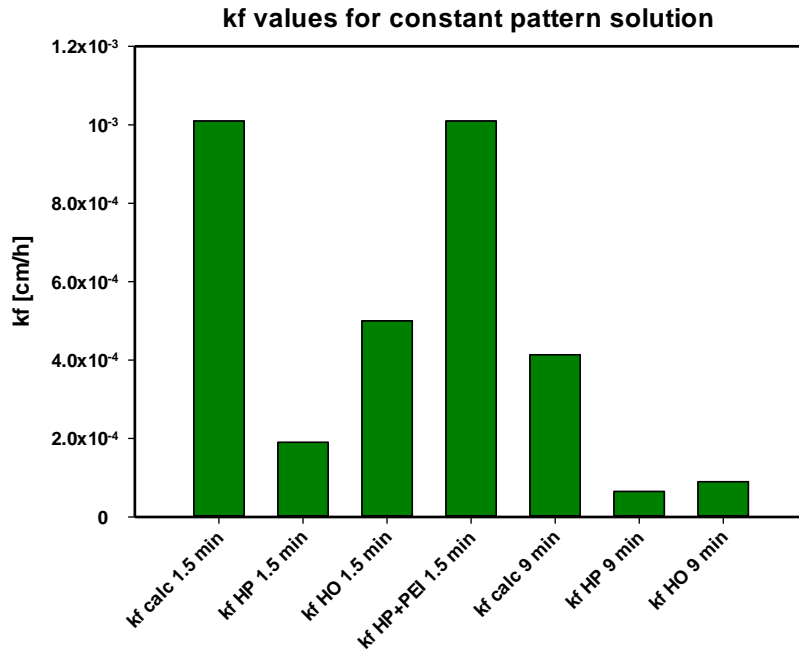
Figure 39: k$_f$ values for constant pattern solution – calculated and fitted

A similar deviation was also observed by Matlschweiger et. al [55]. In their investigation k$_f$ of GFP was one order of magnitude lower in a mixture adsorption with thyroglobulin compared to a pure GFP solution on a Q Sepharose FF gel. They showed that GFP had to diffuse through a thyroglobulin layer on the outer edge of the resin particles which acted like a thin film decelerating protein uptake. In this investigation, it is suspected that DNA or endotoxin or both are responsible for this lowered film mass transfer in the same way. This becomes evident by the evaluation of the SDS PAGE of the elution peaks which are shown in Figure 40. In particular, the comparison of the HP and the HP+PEI at 1.5 min supports this conclusion as no major difference were seen in terms of protein levels. The main difference is the strong depletion of DNA and endotoxin after PEI treatment. For the HO there cannot be made a clear statement, since the elution peaks also showed other proteins, which adsorb with the GFP.
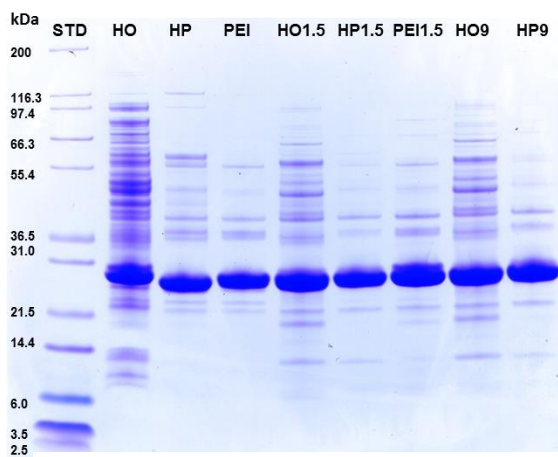
Figure 40: SDS PAGE: diafiltrated HO, HP and HP+PEI (PEI); elution peaks at 1.5 min HO, HP, HP+PEI; elution peaks at 9 min HO, HP

Also, the highest pore diffusion coefficient was observed for the HP+PEI which was approx. 2 times the De of HP at 1.5 min residence time. The results of the fitted De values are summarised in Table 24 and graphically represented in Figure 41. The higher pore diffusion coefficient could also be explained with the strong depletion of DNA and endotoxin for HP+PEI compared to HP. Also for HO, it is suspected that DNA and endotoxin have an dominating influence on the effective pore diffusion coefficient but it cannot be verified that these two components are the only ones which reduce the mass transfer into the pores, since also other components were found in the elution peak.

Table 24: Results of De for HO, HP and HP+PEI

residence time [min]	De [cm^2/s]		
	HO	HP	HP+PEI
1.5	$5*10^{-8}$	$2.1*10^{-7}$	$4.3*10^{-7}$
9	$2.5*10^{-8}$	$1.2*10^{-7}$	
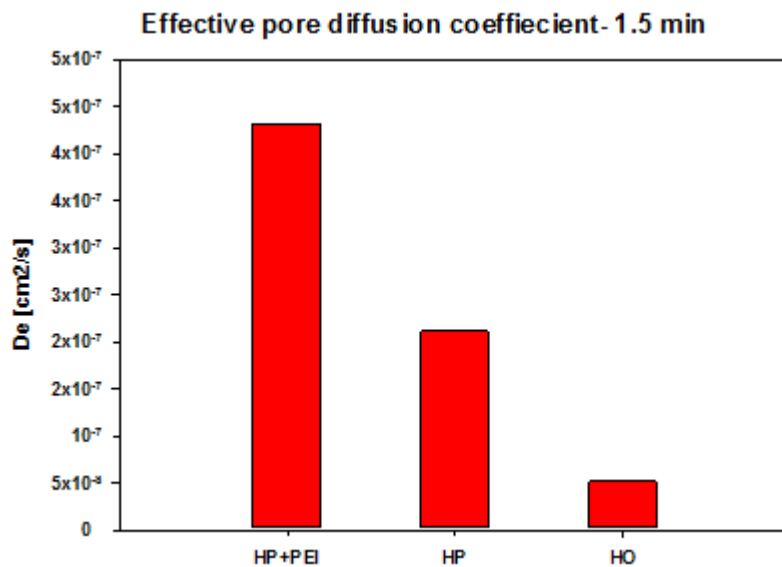
Figure 41: Results of De for HO, HP and HP+PEI at 1.5 min residence time

4. Summary and Conclusion

In this study, it was shown that different operating conditions in HPH have influence on endotoxin and DNA release from *E .coli*. With increasing operating pressure, the release of endotoxin increased leading to a maximum level of 1.2 million EU/mL. Furthermore it was shown that a second passage led to additional endotoxin release. This behaviour was also observed for DNA. However in contrast to endotoxin release, the highest release was not obtained at the highest operating pressure. It is suspected that this is caused by the formation of small DNA oligomers after HPH which cannot be detected with the used detection assay.

Incubation of homogenates with PEI led to a strong depletion of DNA, endotoxin and turbidity by polymer bridging of negatively charged particles and soluble molecules. At a PEI concentration of 0.2% (w/v) most of DNA and endotoxins were depleted and these levels remained constant also after further PEI addition. In case of upscale experiment, it was shown that it is important to choose the PEI concentration on the lower limit. Higher PEI concentrations led to a high increase of turbidity after ultra- and especially diafiltration. A possible explanation is, that surplus- and weakly bound PEI is released into the supernatant and the conductivity change during diafiltration reinforces this mechanism leading to precipitation and membrane fouling

Negatively charged DNA and endotoxins apparently have a great influence on the adsorption behaviour of GFP on a CaptoQ resin. By the use of adsorption isotherms, it was shown that GFP is displaced from the resin at higher GFP concentration when using a diafiltrated homogenate and a diafiltrated heat-treated homogenate as starting solutions. In both cases a high increase of the binding capacity of DNA and endotoxin was observed when the binding capacity of GFP started to drop. In contrast, the PEI treated samples didn`t show this displacement and furthermore highly favourable isotherms with binding capacities of 250 mg/mL were obtained. Especially the comparison of heat-treated and heat- and PEI treated homogenates supports the assumption that DNA and endotoxins are the displacing components where the big difference is the strong depletion of DNA and endotoxins from the latter. The question that remains is the actual shape of the isotherms of DNA and endotoxins. Due to the obtained results, it is hypothesised that DNA and endotoxins show non Langmuir adsorption behaviour but with the used detection and quantification methods it was not possibly to verify this. In batch adsorption experiments, it was shown that the observed displacement is a very slow process. Surprisingly the adsorption of DNA was very fast and could be explained by fragmentation after HPH. Endotoxin also showed fast initial adsorption but also continuously increasing binding capacity. A possible explanation is based on the arrangement of endotoxins in solution. Free endotoxin monomers diffuse fast into the resin

pores, whereas endotoxin aggregates are excluded and bound on the outer surface of the resin particles. It is possible that these aggregates release monomers, which are then able diffuse into the pores and displace the GFP. In column break-through experiments it was shown, that DNA and endotoxins have distinct adsorption behaviour. While for DNA almost no breakthrough was observed, endotoxins showed higher initial and also complete break-through at the end of the loading step. Higher flow rate led to a higher break-through in both cases. The break-through curves were evaluated using the constant pattern solution for film and pore diffusion. The heat- and PEI treated sample not only showed a much higher $DBC_{10\%}$ but also a higher D_e and k_f compared to the homogenate and the heat-treated homogenate. Especially the comparison of the heat- and PEI treated homogenate and the heat-treated homogenate led to the assumption that DNA and endotoxin reduce the film and pore diffusion.

To sum up, DNA and endotoxin apparently have a great impact on adsorption behaviour of GFP. Further investigations would have to be made to verify the assumption that DNA and endotoxins show actually type III adsorption behaviour. Another question which could not be solved is the degree of fragmentation of the DNA and the actual arrangement of endotoxins after HPH and especially how far the smaller fragments diffuse into the resin particles. This question could be solved for the DNA by the use of the Hoechst dye and confocal microscopy analysis. For endotoxins the quantification is based on a reaction cascade and a method that stains endotoxin molecules directly is not available right now.

5. List of Figures

6. List of Tables

7. List of Equations

8. Literature

[1]   M. N. Baeshen *et al.*, "Production of Biopharmaceuticals in E. coli: Current Scenario and Future Perspectives," *J. Microbiol. Biotechnol.*, vol. 25, no. 7, pp. 953–962, Jul. 2015.

[2]   N. Ferrer-Miralles, J. Domingo-Espín, J. Corchero, E. Vázquez, and A. Villaverde, "Microbial factories for recombinant pharmaceuticals," *Microb. Cell Fact.*, vol. 8, no. 1, p. 17, Mar. 2009.

[3]   J. R. Swartz, "Advances in Escherichia coli production of therapeutic proteins," *Curr. Opin. Biotechnol.*, vol. 12, no. 2, pp. 195–201, Apr. 2001.

[4]   F. C. Neidhardt, *Physiology of the bacterial cell : a molecular approach /.* Sunderland, Mass. : Sinauer Associates, 1990.

[5]   G. Carta and A. Jungbauer, *Protein Chromatography Process Development and Scale-Up.* WILEY-VCH Verlag GmbH & Co. KGaA, Weinheim, 2010.

[6]   M. Sakata, M. Nakayama, T. Fujisaki, S. Morimura, M. Kunitake, and C. Hirayama, "Chromatographic Removal of Host Cell DNA from Cellular Products Using Columns Packed with Cationic Copolymer Beads," *Chromatographia*, vol. 62, no. 9–10, pp. 465–470, Nov. 2005.

[7]   "Report on WHO Expert Commitee on Biological Standardization (1977) WHO Weekly Epidemeological Record 72:141-145," 1977.

[8]   O. Fritsche, *Mikrobiologie.* 2016.

[9]   H. Niki, Y. Yamaichi, and S. Hiraga, "Dynamic organization of chromosomal DNA in Escherichia coli.," *Genes Dev.*, vol. 14, no. 2, pp. 212–23, Jan. 2000.

[10]   T. Paustian, "Nucleic Acid Structure," 2001. [Online]. Available: http://lecturer.ukdw.ac.id/dhira/BacterialStructure/NucleicAcids.html. [Accessed: 30-Oct-2018].

[11]   P. Yakovchuk, E. Protozanova, and M. D. Frank-Kamenetskii, "Base-stacking and base-pairing contributions into thermal stability of the DNA double helix.," *Nucleic Acids Res.*, vol. 34, no. 2, pp. 564–74, 2006.

[12]   F. B. Anspach, "Endotoxin removal by affinity sorbents," *J. Biochem. Biophys. Methods*, vol. 49, no. 1–3, pp. 665–681, Oct. 2001.

[13]   C. Erridge, E. Bennett-Guerrero, and I. R. Poxton, "Structure and function of

lipopolysaccharides," *Microbes Infect.*, vol. 4, no. 8, pp. 837–851, Jul. 2002.

[14]   Y. Ogikubo *et al.*, "Evaluation of the bacterial endotoxin test for quantification of endotoxin contamination of porcine vaccines," *Biologicals*, vol. 32, no. 2, pp. 88–93, Jun. 2004.

[15]   N. Ohno and D. C. Morrison, "Lipopolysaccharide interaction with lysozyme. Binding of lipopolysaccharide to lysozyme and inhibition of lysozyme enzymatic activity.," *J. Biol. Chem.*, vol. 264, no. 8, pp. 4434–41, Mar. 1989.

[16]   M.-F. Lin, C. Williams, M. V. Murray, and P. A. Ropp, "Removal of lipopolysaccharides from protein–lipopolysaccharide complexes by nonflammable solvents," *J. Chromatogr. B*, vol. 816, no. 1–2, pp. 167–174, Feb. 2005.

[17]   C. R. H. Raetz, "Biochemistry of Endotoxins," *Annu. Rev. Biochem.*, vol. 59, no. 1, pp. 129–170, Jun. 1990.

[18]   K. Hou and R. Zaniewski, "Endotoxin removal by anion- exchange polymeric matrix," *Biotechnol. Appl. Biochem.*, vol. 12, no. 3, pp. 315–324, Jun. 1990.

[19]   M. L. DePamphilis, "Dissociation and reassembly of Escherichia coli outer membrane and of lipopolysaccharide, and their reassembly onto flagellar basal bodies.," *J. Bacteriol.*, vol. 105, no. 3, pp. 1184–99, Mar. 1971.

[20]   Y. Wang and R. I. Hollingsworth, "An NMR Spectroscopy and Molecular Mechanics Study of the Molecular Basis for the Supramolecular Structure of Lipopolysaccharides †," *Biochemistry*, vol. 35, no. 18, pp. 5647–5654, Jan. 1996.

[21]   F. H. Johnson, O. Shimomura, Y. Saiga, L. C. Gershman, G. T. Reynolds, and J. R. Waters, "Quantum efficiency of *Cypridina* luminescence, with a note on that of *Aequorea*," *J. Cell. Comp. Physiol.*, vol. 60, no. 1, pp. 85–103, Aug. 1962.

[22]   O. SHIMOMURA, F. H. JOHNSON, and Y. SAIGA, "Extraction, purification and properties of aequorin, a bioluminescent protein from the luminous hydromedusan, Aequorea.," *J. Cell. Comp. Physiol.*, vol. 59, pp. 223–39, Jun. 1962.

[23]   A. Kumar, "Green Fluorescent Protein and Their Applications in Advance Green Fluorescent Protein and Their Applications in," vol. 01, no. January, pp. 42–46, 2016.

[24]   B. P. Cormack, R. H. Valdivia, and S. Falkow, "FACS-optimized mutants of the green fluorescent protein (GFP)," *Gene*, vol. 173, no. 1, pp. 33–38, Jan. 1996.

[25]   D. D. Song and N. A. Jacques, "Cell Disruption ofEscherichia coliby Glass Bead Stirring for the Recovery of Recombinant Proteins," *Anal. Biochem.*, vol. 248, no. 2, pp. 300–

301, Jun. 1997.

[26]   "E.   coli   Lysis   by   Homogenization."   [Online].   Available: https://www.gea.com/en/applications/pharma/liquid-dosage/liquid-dosage_cell-disruption_e-coli.jsp. [Accessed: 31-Oct-2018].

[27]   P. M. Doran, *Bioprocess Engineering Principles*, 2. Elsevier, 2013.

[28]   G. Bylund, *Dairy processing handbook*. Tetra Pak Processing Systems AB, 2015.

[29]   R. Lander, W. Manger, M. Scouloudis, A. Ku, C. Davis, and A. Lee, "Gaulin Homogenization: A Mechanistic Study," *Biotechnol. Prog.*, vol. 16, no. 1, pp. 80–85, Feb. 2000.

[30]   C. Zartler, "Heatprecipitation of homogenates : Scale-up study," 2017.

[31]   H. H. Wong, B. K. O'Neill, and A. P. J. Middelberg, "A mathematical model for Escherichia coli debris size reduction during high pressure homogenisation based on grinding theory," *Chem. Eng. Sci.*, vol. 52, no. 17, pp. 2883–2890, Sep. 1997.

[32]   W. J. Kelly and K. R. Muske, "Optimal operation of high-pressure homogenization for intracellular product recovery," *Bioprocess Biosyst. Eng.*, vol. 27, no. 1, pp. 25–37, Dec. 2004.

[33]   G. Trefalt and M. Borkovec, "Overview of DLVO Theory," *Lab. Colloid Surf. Chem. Univ. Genebra*, pp. 1–10, 2014.

[34]   R. G. Harrison, P. Todd, S. R. Rudge, and D. P. Petrides, *Bioseperations Science and Engineering*. Oxford University Press, 2003.

[35]   J. R. Lepock, "Measurement of protein stability and protein denaturation in cells using differential scanning calorimetry," *Methods*, vol. 35, no. 2, pp. 117–125, Feb. 2005.

[36]   A. V. Hill, "The heat produced in contracture and muscular tone," *J. Physiol.*, vol. 40, no. 5, pp. 389–403, Jul. 1910.

[37]   K. Ghosh and K. Dill, "Cellular proteomes have broad distributions of protein stability.," *Biophys. J.*, vol. 99, no. 12, pp. 3996–4002, Dec. 2010.

[38]   S. Kwon, Y. Jung, and D. Lim, "Proteomic analysis of heat-stable proteins in Escherichia coli.," *BMB Rep.*, vol. 41, no. 2, pp. 108–11, Feb. 2008.

[39]   M. Fink, "Clarification of E . coli homogenates by precipitation."

[40]   J. R. Hutton, "Renaturation kinetics and thermal stability of DNA in aqueous solutions

of formamide and urea.," *Nucleic Acids Res.*, vol. 4, no. 10, pp. 3537–55, Oct. 1977.

[41]   "Thermal denaturation of DNA molecules: A comparison of theory with experiment," *Phys. Rep.*, vol. 126, no. 2, pp. 67–107, Sep. 1985.

[42]   K. Tsuji, A. R. Lewis, and N. Kasai, "Dry-heat destruction of lipopolysaccharide: mathematical approach to process evaluation.," *Appl. Environ. Microbiol.*, vol. 36, no. 5, pp. 715–9, Nov. 1978.

[43]   T. Miyamoto, S. Okano, and N. Kasai, "Inactivation of Escherichia coli endotoxin by soft hydrothermal processing.," *Appl. Environ. Microbiol.*, vol. 75, no. 15, pp. 5058–63, Aug. 2009.

[44]   GE Healthcare, "Cross Flow Filtration Method Handbook," *Broch. 29-0850-76 AB 03/2014 a1675*, pp. 1–80, 2014.

[45]   R. Hahn, "Methods for characterization of biochromatography media," *J. Sep. Sci.*, vol. 35, no. 22, pp. 3001–3032, 2012.

[46]   J. R. Lakowicz, "Introduction to Fluorescence," in *Principles of Fluorescence Spectroscopy*, Boston, MA: Springer US, 2006, pp. 1–26.

[47]   W. Su and X. Ding, "Methods of Endotoxin Detection," *J. Lab. Autom.*, vol. 20, no. 4, pp. 354–364, Aug. 2015.

[48]   R. Nachum and R. N. Berzofsky, "Chromogenic Limulus amoebocyte lysate assay for rapid detection of gram-negative bacteriuria.," *J. Clin. Microbiol.*, vol. 21, no. 5, pp. 759–63, May 1985.

[49]   "Advantages of recombinant Factor C based endotoxin testing - EPM Magazine," *European PHARMACEUTICAL manufacturer*, Nov-2015.

[50]   Biorad, "Fluorescent DNA Quantitation Kit Instruction Manual Catalog Number," no. 170, p. 15, 2000.

[51]   Hach company, "DETERMINATION OF TURBIDITY BY NEPHELOMETRY - Hach method 8195," no. December, pp. 1–12, 1997.

[52]   Lawler, "Turbidimetry and Nephelometry," pp. 343–351, 2005.

[53]   N. Saraswathy and P. Ramalingam, *Concepts and techniques in genomics and proteomics*. Woodhead Pub, 2011.

[54]   C. Hirayama, M. Sakata, M. Nakamura, H. Ihara, M. Kunitake, and M. Todokoro, "Preparation of poly(ε-lysine) adsorbents and application to selective removal of

lipopolysaccharides," *J. Chromatogr. B Biomed. Sci. Appl.*, vol. 721, no. 2, pp. 187–195, Jan. 1999.

[55]   A. Matlschweiger, P. Fuks, G. Carta, and R. Hahn, "Hindered diffusion of proteins in mixture adsorption on porous anion exchangers and impact on flow-through purification of large proteins," *J. Chromatogr. A*, 2018.

9. Appendix
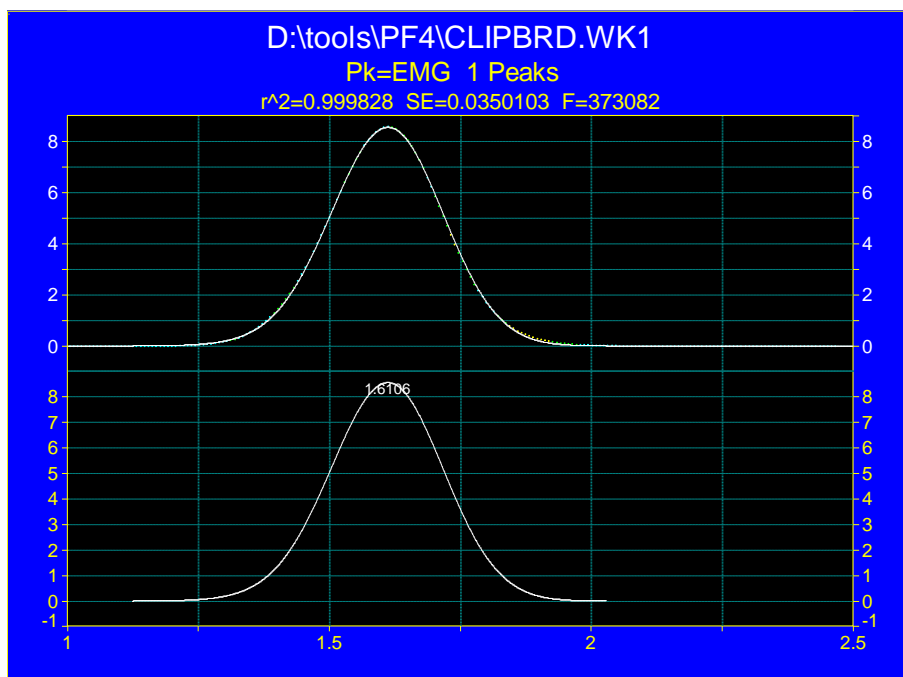
Figure 42: Evaluation of packaging performance CaptoQ

Fitted Parameters							
r^2 Coef Det	DF Adj r^2	Fit Std Err	F-value				
0.99982849	0.99982489	0.03501034	373080				
Peak	Type	a0	a1	a2	a3		
1	EMG	2.30634508	1.64627433	0.100924	-0.03987		
Measured Values							
Peak	Type	Amplitude	Center	FWHM	Asym50	FW Base	Asym10
1	EMG	8.56347207	1.61056137	0.251878	0.974581	0.508487	0.948179
Peak	Type	Anlytc Area	% Area	Int Area	% Area	Centroid	Moment2
1	EMG	2.30634508	100	2.306339	100	1.606402	0.011775
Total	2.30634508	100	2.30633924	100			
Chromatographic Analysis							
Peak	Type	Nmoment	NGauss	FW Base	Asym10	Resolution	
1	EMG	219.1616	226.720465	0.508487	0.948179		
Analysis of Variance							
r^2 Coef Det	DF Adj r^2	Fit Std Err					
0.99982849	0.99982489	0.03501034					
Source	Sum of Squares	DF	Mean Square	F			
Regr	1371.8868	3	457.29561	373082			
Error	0.23533905	192	0.001225724				
Total	1372.1222	195					
Details of Fit							
Set Convergence	State	Iterations	Minimization	Extent			
0.000001	Converged	10	Lorentzian	1/1			
Curvature Matrix	Constraints	Violated					
Sparse-Roots	25.0000-5.00000-50.0000- None - None	0					

Table 25: Results of the Adsorption Isotherms for the diafiltrated Homogenate

GFP supernatant [mg/mL]	mgGFP/mL resin	DNA supernatant [mg/mL]	mgDNA/mL resin	Endotoxin supernatant [mg/mL]	mgEndotoxin/mL resin
0.00	23	0.20	2	0.020	1
0.03	68	0.29	5	0.022	2
0.33	92	0.35	7	0.026	2
2.84	89	0.31	11	0.025	3
7.43	36	0.24	24	0.012	7
8.53	20	0.25	48	0.014	14

Table 26: Results of the Adsorption isotherms for the diafiltrated Heat-precipitate

GFP supernatant [mg/mL]	mgGFP/mL resin	DNA supernatant [mg/mL]	mgDNA/mL resin	Endotoxin supernatant [mg/mL]	mgEndotoxin/mL resin
0.00	152.8	0.012	1.1		
0.02	168.6	0.011	1.3		
0.09	193.1	0.012	1.5	0.063	1.1
0.82	205.6	0.014	1.6	0.060	1.3
2.38	199.3	0.015	1.9	0.059	1.6
4.13	185.3	0.018	2.2	0.022	3.1
6.08	157.9	0.021	2.6	0.013	4.2
7.88	121.9	0.021	3.5	0.008	6.0
9.53	64.7	0.021	5.2	0.025	7.6
10.26	36.7	0.025	10.0	0.036	13.8

Table 27: Results of the Adsorption Isotherms: Heat-precipitate +0.2%PEI and Homogenate + 0.3%PEI

Heat-precipitate + 0.2%PEI			
GFP supernant [mg/mL]	mgGFP/mL resin	DNA supernatant [mg/mL]	mgDNA/ mL resin
0.00	116		
0.00	158	u.l*	u.l
0.00	203	u.l	u.l
0.00	208	u.l	u.l
0.23	215	0.008	0.242
1.41	230	0.011	0.209
3.25	242	0.012	0.235
4.98	230	0.014	0.236
6.03	232	0.015	0.231
7.48	237	0.016	0.337
8.53	251	0.016	0.622
Homogenate + 0.3%PEI			
GFP supernant [mg/mL]	mgGFP/mL resin	DNA supernatant [mg/mL]	mgDNA/mL resin
0.01	251	0.010	0.278
0.95	258	0.011	0.291
2.81	270	0.013	0.300
4.01	266	0.015	0.299
5.72	256	0.017	0.346
7.13	252	0.019	0.367
8.83	234	0.020	0.612

*under limit of detection

Table 28: Results of the Adsorption Isotherms: ultrafiltrated and diluted Heat-precipiate+0.22%PEI and Homogenate+0.2%PEI

Heat-precipitate + 0.22%PEI		Homogenate + 0.2%PEI	
GFP supernant [mg/mL]	mgGFP/mL resin	GFP supernant [mg/mL]	mgGFP/mL resin
3.9	147	3.96	118
1.8	153	2.39	115
0.34	137	1.12	107
0.098	102	0.158	98
0.037	70	0.028	68

Table 29: Results of Batch adsorption - HO and HP

HO						
Time [min]	GFP sn [mg/mL]	mgGFP/mL resin	DNA sn [mg/mL]	mgDNA/mL resin	ET sn [mg/mL]	mgET/mL resin
0.5	8.44	21	0.63	16		
1	8.05	43	0.21	39	0.199	4.5
2	7.76	59	0.15	42		
15	6.96	103	0.14	43		
30	6.93	104	0.12	44		
60	6.87	108	0.11	44	0.196	4.7
120	7.19	90	0.11	44		
180	7.37	80	0.11	45		
360	7.65	65	0.11	45	0.165	6.43
490	7.90	51	0.11	45		
620	8.47	20	0.09	45		
690	8.69	8	0.06	47	0.112	9.38
Heat-treated homogenate						
Time [min]	GFP sn [mg/mL]	mgGFP/mL resin	DNA sn [mg/mL]	mgDNA/mL resin	ET sn [mg/mL]	mgET/mL resin
0.5	8.66	58	0.063	10		
1	8.39	73	0.012	13	0.208	3.6
5	7.51	120	0.012	13		
15	6.93	154	0.011	13		
30	6.65	170	0.009	13		
60	6.65	170	0.011	13	0.186	4.8
120	6.65	169	0.010	13		
180	6.65	170	0.009	13		
240	6.65	170	0.010	13		
300	6.84	170	0.009	13		
470	7.16	142	0.010	13		
690	7.61	117	0.009	13	0.165	5.9
1440	8.29	79	0.005	13	0.088	10.2

*sn = supernatant, ET = Endotoxin

Table 30: Results of Batch Adsorption: HP+PEI

HP+ PEI		
Time [min]	GFP sn [mg/mL]	mgGFP/mL resin
0.5	7.95	107
1	7.56	139
5	7.20	168
15	6.93	191
30	6.27	245
60	5.79	284
120	5.68	293
240	5.60	300
1200	5.63	297
1440	5.54	304

Table 31: DNA and Endotoxin in breakthrough and Elution Homogenate

	1.5 min residence time		9 min residence time	
Load Voume [mL]	**cf/c0 DNA**	**cf/c0 Endotoxin**	**cf/c0 DNA**	**cf/c0 Endotoxin**
0.76	0.02		0.01	
1.76	0.05		0.13	
2.76	0.09		0.12	
3.76	0.10		0.12	
4.76	0.11	0.44	0.12	0.24
5.76	0.11		0.12	
6.76	0.11		0.10	
7.76	0.12		0.12	
8.76	0.12		0.11	
9.76	0.12		0.12	
10.76	0.13	0.43	0.12	0.37
11.76	0.13		0.12	
12.76	0.13		0.11	
13.76	0.14	0.81	0.13	0.73
14.76	0.14		0.10	
15.76	0.14		0.07	
16.76	0.15	0.80	0.12	0.67
17.76	0.15		0.11	
18.76	0.15		0.12	
Sample at elution	**DNA [mg/mL]**	**Endotoxin [mg/mL]**	**DNA [mg/mL]**	**Endotoxin [mg/mL]**
1 mL 30%B*	0.08		0.02	
2 mL 30%B	0.102		0.09	
3 mL 30%Br	0.09	0.022	0.10	0.014
4 mL 30%B	0.05		0.06	
5 mL 30%B	0.04		-	-
1 mL 100%B	0.08		0.02	
2 mL 100%B	0.07	0.031	0.02	0.021
3 mL 100%Br	0.04		0.02	
4 mL 100%Br	-	-	0.03	

*elution Buffer

Table 32: DNA and Endotoxin in breakthrough and Elution – heat-treated homogenate

| Load Voume [mL]	1.5 min residence time		9 min residence time	
	cf/c0 DNA	cf/c0 Endotoxin	cf/c0 DNA	cf/c0 Endotoxin
0.76	0.00		0.00	
1.76	0.00		0.00	
2.76	0.01		0.01	
3.76	0.02		0.02	
4.76	0.03		0.02	
5.76	0.03		0.02	
6.76	0.04		0.03	
7.76	0.04		0.03	
8.76	0.05		0.03	
9.76	0.05		0.03	
10.76	0.06	0.40	0.03	0.34
11.76	0.06		0.03	
12.76	0.06		0.03	
13.76	0.07		0.03	
14.76	0.07		0.03	
15.76	0.08	0.73	0.04	0.56
16.76	0.08		0.04	
17.76	0.09		0.04	
18.76	0.10		0.04	
19.76	0.11		0.06	
20.76	0.12	0.83	0.06	0.60
21.76	0.12		0.06	
22.76	0.13		0.07	
23.76	0.14		0.07	
24.76	0.15		0.07	
25.76	0.15	1.02	0.07	0.81
Sample at elution	**DNA [mg/mL]**	**Endotoxin [mg/mL]**	**DNA [mg/mL]**	**Endotoxin [mg/mL]**
1 mL 30%B*	0.05		0.01	
2 mL 30%B	0.04		0.03	
3 mL 30%Br	0.03		0.03	
4 mL 30%B	0.02	0.014	0.02	0.015
1 mL 100%B	0.95		0.13	
2 mL 100%B	0.64		0.39	
3 mL 100%Br	0.34	0.021	0.58	0.049

Figure 43: experimental vs fitted curves – break-through HO, HP, HP+PEI